DEVELOPMENT IN QUALITY CONTROL OF CONCRETE DURING CONSTRUCTION

W. Wilk and G. Dobrolubov, Betonstrassen AG, Switzerland; and
B. Romer, LPM Laboratory, Switzerland

New methods of quality control of concrete during pavement construction have successfully been carried out in Switzerland on all main road projects since 1969. A combined quantitative and qualitative microscopic analysis has been carried out on thin slices of 2-day-old concrete in more than 800 tests. Quantitative analysis determines the frost-salt (F-S) resistance. In addition to the spacing factor, nine other factors are being considered. The evaluation of F-S resistance foresees a subdivision in five groups according to the durability factor. The qualitative, morphological control analysis is done on the same slice and at the same time the quantitative analysis is carried out. The morphological quality control determines precisely the faults in the concrete as well as their causes. It also makes it possible to rectify these faults during further construction. Concrete with medium or low F-S resistance (according to the quantitative analysis) or with a high percentage of morphological faults (disturbance factor ≥ -10) is controlled by a frost-thaw-salt (F-T-S) resistance test with rapid cycles. This new Dobrolubov-Romer (D-R) method makes rapid testing of concrete possible (500 cycles within a fortnight). Practical application of control on site during construction is demonstrated.

•SEVERAL control examinations have been applied during concrete highway construction in Switzerland since 1969 and are discussed in the following.

AIR CONTENT DETERMINATION IN FRESH CONCRETE

The air content of fresh concrete is determined immediately before compaction. Distributed concrete from a vibrating slab and a pressure equalizing apparatus, Tonindustrie Berlin, are used for the determination. According to Swiss specifications (SNV-640478), air-entrained concrete must contain between 4 and 6 percent air by volume; therefore total air content (e.g., compaction and entrained air pores) is measured.

The results depend on the compaction of the concrete in the apparatus and can vary up to 2 percent by volume. The purpose of the investigation is to detect faults in the placing so that the necessary corrections can be implemented. Insufficient air content in fresh concrete can occur through (a) absence or an insufficient dose of an air-entraining agent, (b) reduction of the mixing time, (c) concrete that is too dry, (d) excessive transportation or waiting time, and (e) different qualities of air-entraining agents.

During concrete road construction, air content of fresh concrete is determined between five and ten times daily. Although the test is meant to serve as a control, it can give no conclusive estimates of the F-S resistance of the concrete.

MICROSCOPIC PORE ANALYTICAL DETERMINATION OF F-S RESISTANCE

For this investigation three 5-cm-diameter cores are taken from the hardened pavement. This can be done after 24 hours in warm conditions, or after 48 hours. One

Publication of this paper sponsored by Committee on Performance of Concrete—Physical Aspects.

core is used for the preparation of two thin sections. The remaining cores are for the 5-day water saturation test A_5 and for the in-vacuum water saturation test A_v. Results of these investigations are available 7 days after concreting. Partial information, without water saturation results, can be given by telephone 3 days after concreting.

Evaluation and judgment of F-S resistance are based on pore analysis and deduced characteristic values. The following values are used in the assessment:

Lf = fresh concrete/air volume, percent;
La = hardened concrete/air volume, percent;
α = mean specific pore surface, mm^{-1};
Pi = number of pores per mm^3 of sample;
L_{300} = volume of pores up to 300 micron diameter, percent;

$$V_1 = \frac{L_{300}}{K_5} \cdot 100, \text{ where } K_5 = A_5 \text{ - gel water;}$$

$$V_2 = \frac{L_{300}}{A_5} \cdot 100;$$

WB_1 = supplementary value = $V_1 \sigma$ kg/cm^2, where σ = flexural strength at 28 days;
WB_2 = supplementary value = $V_2 \sigma$ kg/cm^2; and
AF = spacing factor in mm (after Powers).

This evaluation is based on Figure 1. Plotting the resulting characteristic values produces a curve. (The dashed line is concrete No. 2 from Highway N1, St. Gallen-Buriet, which lies within the limits of one of the five F-S resistance groups. Concrete No. 2 has a high F-S resistance.)

The five groups depend on the resistance factor WFT_E—the durability factor—defined in ASTM C 666-B. Groups with a very high and high F-T-S resistance correspond to a WFT_E value between 100 and 80 percent; a medium F-T-S resistance to between 80 and 50 percent; and a low to very low F-T-S resistance to between 50 and 20 percent (1). Consequently a concrete with a high characteristic value should, after 200 F-T-S cycles of the D-R method, show a reduction of at most 20 percent (WFT_E = 80 percent) in the modulus of elasticity. This F-T-S resistance rating makes a comparison with many American and other research studies possible. It also permits F-T-S resistance resulting from characteristic values to be checked by using the effective resistance factors obtained from the F-T-S test (D-R). Comparative investigations have shown that the morphological characteristics of the concrete can, under circumstances, have considerable influence on the F-T-S resistance. This correlation principle will be discussed later.

MICROSCOPIC MORPHOLOGICAL QUALITATIVE CONTROL OF CONCRETE

Microscopic quantitative (pore analytical) and qualitative (morphological) control of concrete is carried out on thin sections made from a concrete core specimen impregnated with special fluorescent dye and examined under a microscope by transmitted ultraviolet (UV) light. This new method makes otherwise undistinct or undetected features visible. (The new preparation technique was responsible for successful development of qualitative and quantitative control methods as well as for the good correlation of these methods with the F-T-S test.)

Preparation Technique

From a concrete core 5 cm in diameter or a laboratory prism 12 by 12 by 36 cm, a small prism specimen 4 by 2 by 1.5 cm is cut. Wherever the original concrete pavement is the object of the test (which usually is the case), it should be one of the prism's faces. The thin section is generally made perpendicular to the concrete surface.

One large face of the prism is ground to a depth of approximately 2 mm to eliminate all possible damages caused by the cutting process and then ground to a completely finished surface. This specimen is then impregnated under vacuum with a special Duroplast polymer. After hardening, the surplus polymer deposit is removed by grinding

Figure 1. Determination of F-S resistance.

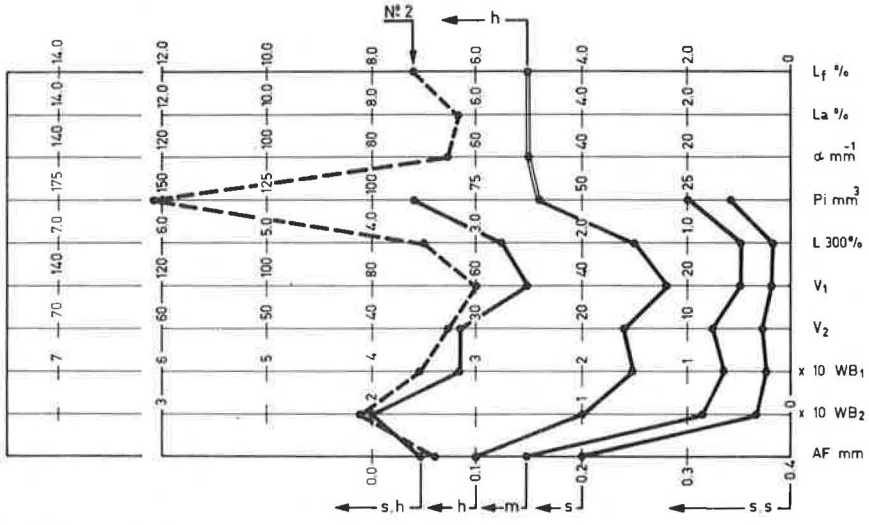

Figure 2. Air-entrained concrete without UV differentiation (x70).

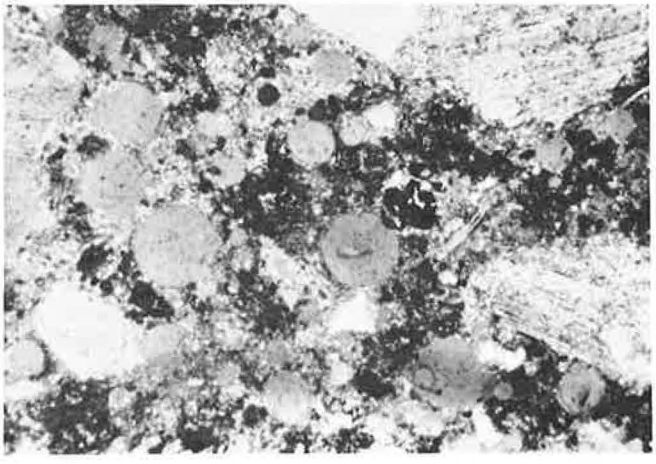

Figure 3. Air-entrained concrete with UV differentiation (x70).

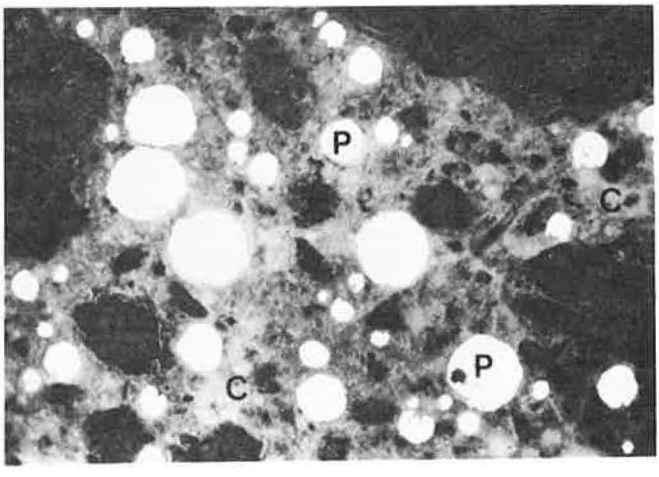

from the finished surface, from which 50 to 100 microns of concrete are ground. On the surface obtained, a protection glass is fixed.

Then the specimen's opposite surface is cut and ground to achieve a thin section 25 microns thick. All "hollow" spaces in the concrete of this thin section are impregnated with a special polymer with a colorful fluorescent tracer. In the case of UV excitement in the microscope, a fluorescent yellow coloring effect is obtained in the hollow spaces—even in those of 1 to 2 microns or smaller. The remaining concrete components are different shades of blue; the aggregates, dark blue; and the cement paste, light blue. Fluorescent coloring makes it possible to localize (by color differentiation) and to evaluate (by color intensity) all hollow spaces.

Evaluation of Morphological Qualitative Control Method

The advantage of this method for making undistinct or undetected features clearly visible appears when Figures 2 and 3 are compared. Their microscopic difference is based on the different colors (yellow and blue), which in this paper are black and white. The differentiation is therefore imperfectly shown. All photomicrographs are magnified and represent an area of approximately 0.33 mm^2 of a thin section of 800 mm^2.

Figure 2 shows an air-entrained concrete—a thin section without UV differentiation seen in a tungsten type of light in a bright field. Figure 3 shows the same cut of concrete—a thin section with UV differentiation by mercury vapor and UV lighting in a dark field. Air voids, capillary porosity of the cement paste, and other yellow (black) hollow spaces are clearly distinct from other blue (white) solid concrete structures.

The possibility of accurate differentiation of some types of (a) voids—P, L, W, and PPP; (b) capillary porosity C of the cement paste (high capillarity = HC, medium-high = m HC, and low = NC), and (c) adherence quality A of the aggregate to a cement paste and to cracks R is shown in Figures 4 through 12.

Figure 4 shows a concrete with an excellent air-void structure P. There are numerous, clearly distinct air voids between 10 and 100 microns in diameter. Figure 5 shows a concrete with entrapped voids L. These are mostly large (of irregular shape, with defined edges) and can be easily differentiated from the entrained air voids that are usually smaller and round. Insufficient compaction, a concrete that is too dry, and long transportation or waiting times before compaction can be the reasons for many entrapped voids in the concrete.

Figure 6 shows a concrete with voids W caused by water concentration. These are similar to the entrapped voids but have unclear edges with dissolved cement paste particles and small aggregates. Rain or any addition of water during transportation, laying, or compaction explains the reason for many of these voids. Similar but clearly distinct voids can be produced by bleeding.

Figure 7 shows a concrete with some voids PPP that have collapsed and agglomerated. A high water-cement ratio, e.g., addition of water during surface finishing, or an inadequate air entrainer may be the reason for void agglomeration.

Figure 8 shows a concrete with low and medium-high capillarity, and Figure 9 shows one with high capillarity. If capillarity of the cement paste is high or variable, it will have a negative influence on frost and F-S resistance. This can be determined through morphological analysis. If the water-cement ratio is too high, excessive capillarity may result. Strong variations in capillarity may be caused by inadequate or short mixing times.

Figures 10 and 11 show concretes with disturbed adherence A between aggregate and cement paste. This can be caused by impurities, peripheral cracks (Fig. 11), or by formation of high capillary porosity in the cement paste surrounding the aggregates (Fig. 10). In all cases these disturbances severely influence the frost and F-S resistance of the concrete and can be detected only through microscopic examination.

Figure 12 shows a concrete with cracks in the cement paste caused by frost damage. An experienced eye can distinguish between frost and fatigue cracks and cracks due to either shrinkage or belated use of the longitudinal finisher.

Figure 4. Concrete with air-void structure (x70.6).

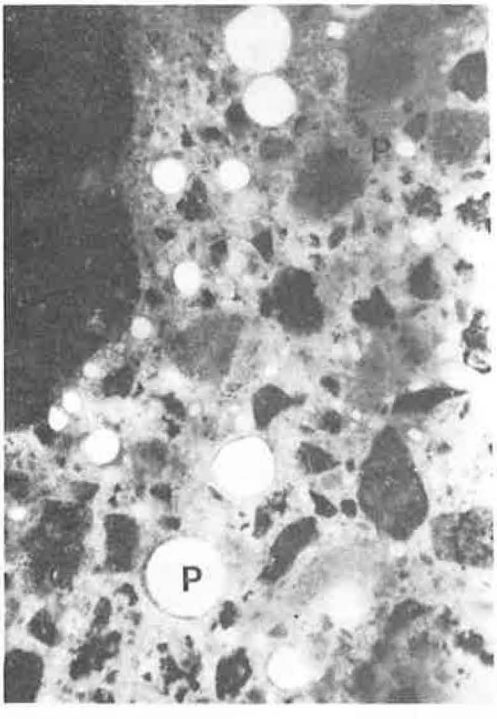

Figure 5. Concrete with entrapped voids (x70.6).

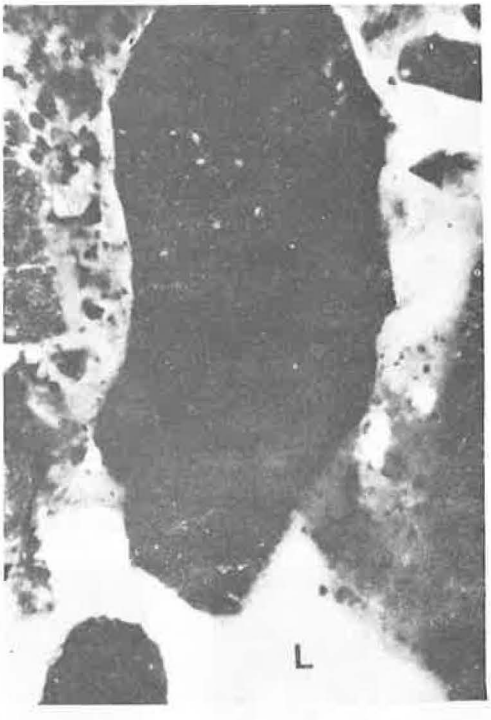

Figure 6. Concrete with voids caused by water (x70.6).

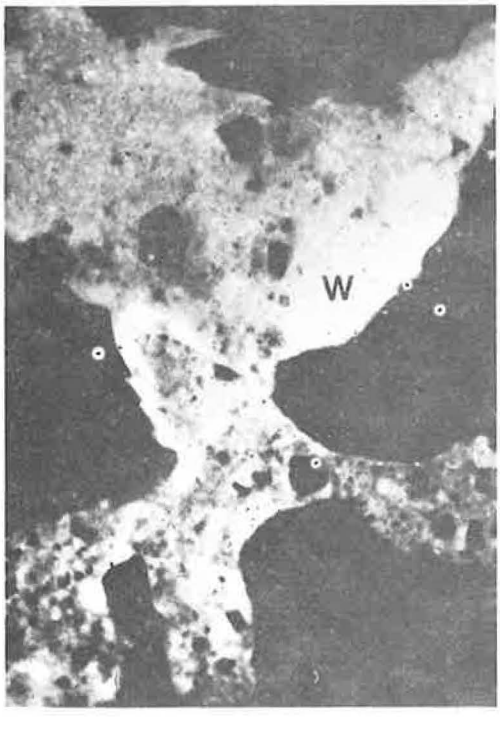

Figure 7. Concrete with collapsed and agglomerated voids (x70.6).

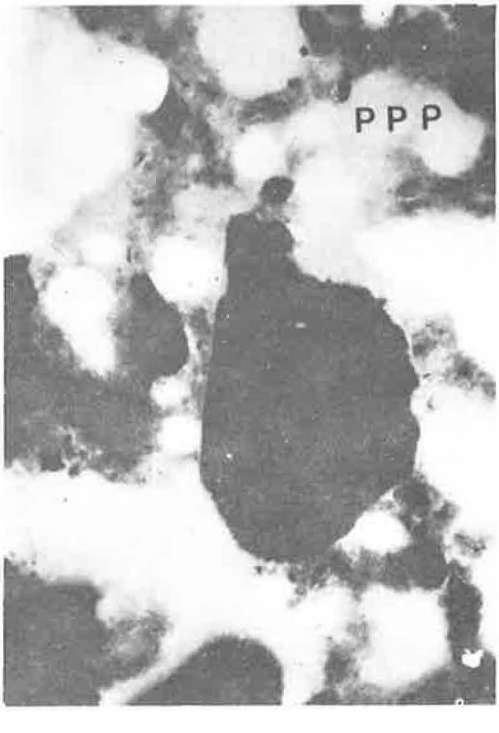

Figure 8. Concrete with low and medium-high capillarity (x50.3).

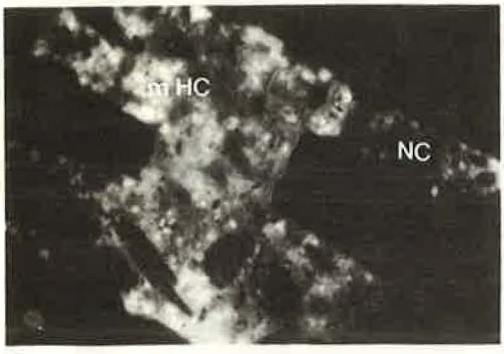

Figure 9. Concrete with high capillarity (x50.3).

Figure 10. Concrete with disturbed adherence caused by high capillarity (x50.3).

Figure 11. Concrete with disturbed adherence caused by peripheral cracks (x50.3).

Figure 12. Concrete with cracks caused by frost damage (x50.3).

Morphological Assessment of the Concrete

Figure 13 shows the procedure used in the morphological assessment of concrete and its evaluation through a disturbance factor. This examination enables one to determine the cause of faults in concrete and allows quick recognition and, in most cases, correction of every negative influence that might appear during construction. A concrete with a total disturbance factor ≤ -5 can be considered completely sound. Larger values call for improvement measures. A disturbance factor ≥ -10 can in some circumstances jeopardize the F-T-S resistance as obtained from the characteristic values of the pore analysis. Investigations have proved that a thin section of 800 mm^2 is a representative sample. A comprehensive pore analysis with a concrete morphology determination (inclusive of preparation) requires about 5 hours, which is less than the 7 to 8 hours required for analysis by the linear transverse principle.

RAPID DETERMINATION OF FROST OR F-T-S RESISTANCE OF CONCRETE WITH D-R METHOD

The deterioration process due to frost or F-S initially causes a loosening of the crystalline paste structure followed by crack development that can lead to destruction of the concrete. This loosening process within the cement paste was proved by microhardness tests. Results of tests on concrete made by the authors show good correlation between the decrease in the modulus of elasticity and the microhardness of the cement paste. Figure 14 shows the relation between the loss in microhardness expressed by the increase of the imprint M, and the loss in modulus of elasticity, both expressed in percent per cycle.

The whole deterioration process taking place within the cement paste [the evaluation of the frost-thaw (F-T) or F-T-S resistance of concrete] may therefore be confined to the evaluation of its cement paste. Small concrete test specimens can thus be used, entailing a shortening of exposure times, which leads to a considerable reduction in overall testing times. For this purpose six prisms 3 by 3 by 6 cm are cut out of cores 15 cm in diameter or out of laboratory prisms of the concrete to be tested.

The rapid method of determination of F-T or F-T-S resistance of concrete has the following characteristics:

1. A fully automatic testing apparatus with extensive programming possibilities;
2. Rapid testing, e.g., 500 cycles in 14 days;
3. A possibility of correlation with other existing test methods by means of the durability factor; and
4. Possibilities of evaluation of F-T-S resistance at different depths (surface, 15, and 30 mm) of the tested concrete.

Test Equipment

The test equipment is compact and fully automatic (Fig. 15). The capacity of each unit allows simultaneous testing of at most 24 concretes with six test prisms 3 by 3 by 6 cm per concrete at a daily average of 50 cycles maximum. With fully automatic controlled canisters, the test specimens are successively immersed into a thawing trough with running water at +20 C and into a freezing trough containing a salt solution at -20 C (Fig. 16). Either calcium chloride at 33 deg Baumé or sodium chloride at 22 deg Baumé may be selected for the salt solution. The time required to freeze a concrete specimen, including the transition from +20 C to -20 C, equals the duration of a cycle.

According to test results, a drop in temperature at the rate of 3.3 C/cm/min and an increase at the rate of 5.3 C/cm/min was established, which for a specimen of 3 by 3 by 6 cm results in 8 min for freezing and 5 min for thawing (Fig. 17). The salt saturation of the concrete specimens can be controlled by adjusting the time of exposure to frost with respect to the time of immersion in the thaw bath.

Test Procedure

The test is carried out on water-saturated specimens; 5 days generally are required for water saturation. The method enables the application of the following test

Figure 13. Morphological assessment of concrete.

By order of: CANTON ST. GALLEN
Object: N1 ST. GALLEN – BURIET
Specimen: SLAB NR. 39

Specimen: SLAB NR. 39	ASSESSMENT	DISTURBANCE FACTOR	Value	REMARKS
POROSITY	see Pore analyssis			
Air Pores				Regular
Pore agglomerations		Frequent	- 2.00	
Voids (Compaction Pores)		less frequent	- 1.50	
Water Voids (Produced by bleeding or addition of Water)	none			
CEMENT PASTE CAPILLARITY				
uniform		low capillarity	- 0.50	
non uniform		non uniform		
CRACKS IN CEMENT PASTE				
Evaluation per 100 mm²	none			
Nr. of Cracks: 0 - 10				
10 - 50				
50 - 150				
fine Cracks				
large Cracks				
Orientation				
AGGREGATES				
Cracks				
Porosity				
ø mm < 0,5	none			
0,5 - 1	none			
1 - 4		few	- 0,25	
> 4		few	- 0,50	
BOND AGGREGATE - CEMENT PASTE				
disturbed				
Through Capillar Disturbance	none			
Through Cracks Disturbance	none			
Voids (Compaction Pores)		some	- 0,50	
HYDRATION	good			

Morphological Assessment: Factor total: - 5,25

By a Dysturbance Factor ≥ - 10 a F.T.S. - Test is recommended

Figure 14. Relation between loss in micro-hardness and loss in modulus of elasticity.

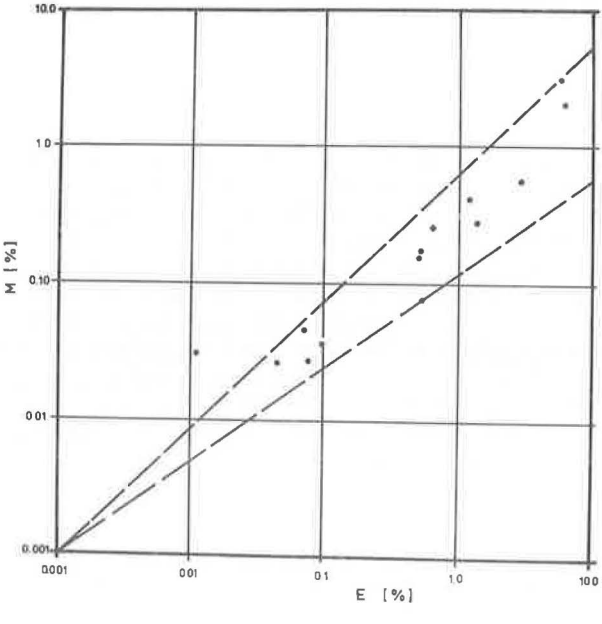

Figure 15. Testing equipment for F-T-S test (D-R).

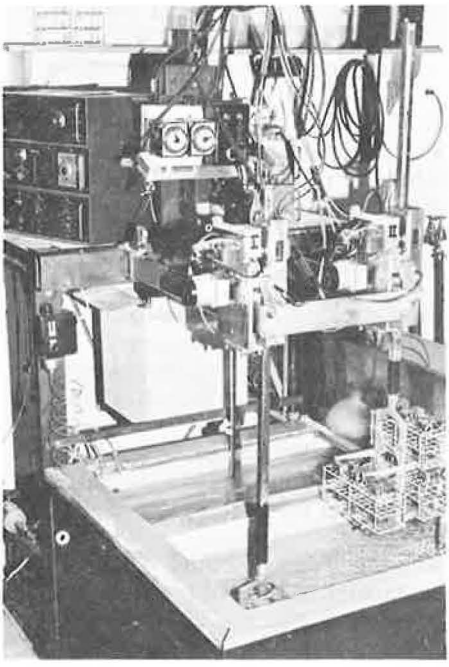

Figure 16. Schematic drawing of functioning test equipment.

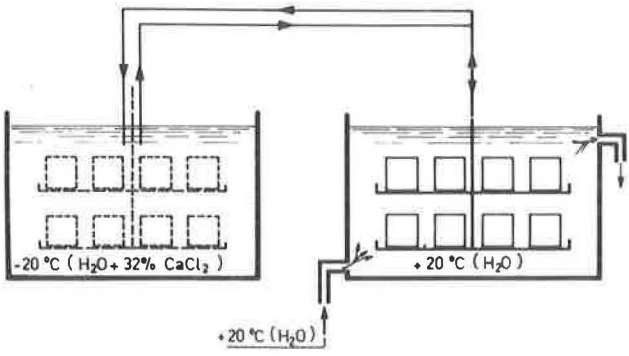

Figure 17. Drop and increase of temperature in center of specimen (in hours).

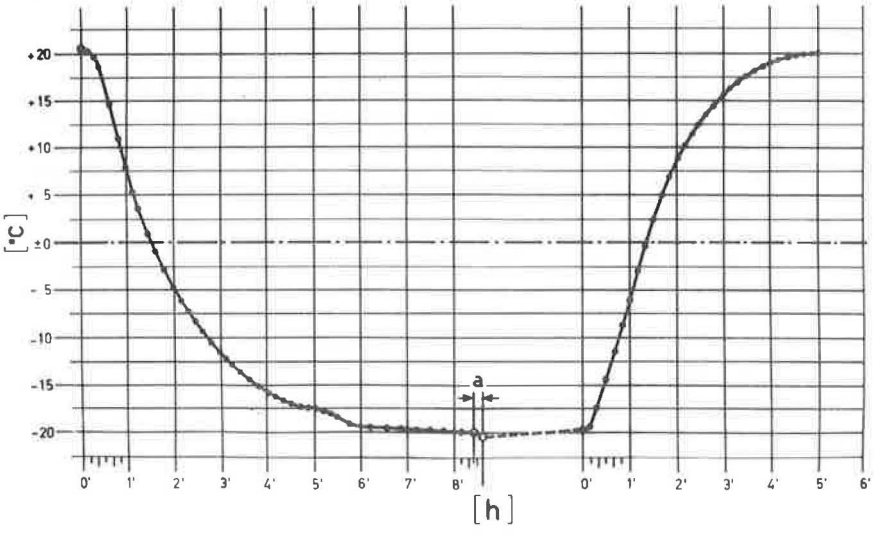

procedures: F-T, F-T-S, and isolated F-T-S.

F-T—This test is carried out on water-saturated specimens in hermetically sealed bags. The salt bath freezes the specimens. The bags impede both salt penetration and specimen drying. Because these bags are used, the exposure time in the frost bath (at -20 C) is extended to 32 min and in the thawing bath (+20 C) to 16 min. With 2 min for transporting the specimens from one bath to the other, total time needed for the course of one cycle is 50 min.

F-T-S—In addition to freezing at -20 C and thawing at +20 C, this test includes temperature shock as well as salt absorption on all sides of the specimen. The temperature shock, which under natural conditions arises from de-icing, is caused (in the test) by the sudden immersion of the specimens into the frost bath. Figure 18 shows the temperature shock in concrete slabs caused by applying de-icing agents such as $CaCl_2$, NaCl, and alcohol. The degree of salt absorption of test specimens is regulated by increasing exposure times in the frost bath.

The degree of saturation of test specimens must approximately correspond to the amount of NaCl in existing concrete pavements under normal conditions. Figure 19 shows the chloride contents of concrete, measured on roads in Switzerland, compared with the chloride contents measured in concrete specimens of 3 by 3 by 6 cm after the F-T-S test.

As a result of various tests, the appropriate exposure time was found to be 2:1, i.e., 20 min exposure in the frost or salt bath at -20 C and 10 min in the thawing water at +20 C. By adding 2 min transporting time, 32 min are needed for a complete F-T-S cycle.

Isolated F-T-S—This test fundamentally corresponds to the F-T-S method. Air insulation of five sides of the specimen (Fig. 20) limits the impact of the cold and the salt to one (unprotected) side only that corresponds to the pavement surface. This test procedure is particularly suitable for testing F-T-S resistance of thin concrete surfaces and allows improvements caused by impregnation or a thin epoxy overlay to be assessed. When the ratio 2:1 is used, the partially insulated test specimens require 50 min to undergo one complete cycle: 32 min exposure to frost, 16 min exposure to thaw, and 2 min transporting time.

Preparation and Measuring Test Specimens

For all three test methods, six test prisms of 3 by 3 by 6 cm are cut off the cores (laboratory prisms). The surface of the original concrete pavement should be one of the prism faces. Each prism specimen is provided with eight measuring marks as shown in Figure 21. Figure 22 shows the cutting of the prism specimens, and Figure 23 shows fastening the measuring marks into the previously bored recesses.

The measurements take place in four phases: The six specimens are measured before the test begins and after either 50, 100, and 200 cycles or after 50, 200, and 400 cycles. The permanent expansions, depending on the number of cycles, are measured in each one of the four phases.

Measuring Axial Expansion L on Four Surfaces

The initial measuring distance between the measuring points is 50 mm. The measuring accuracy is 0.02 percent of the initial length (Fig. 24):

$$L = \frac{L_1 + L_2 + L_3 + L_4}{4}$$

Measuring Transverse Expansion Q Perpendicular to Prism Axis

The initial measuring distance between the measuring points is 30 mm. The measuring accuracy is 0.033 percent of the initial length (Fig. 25):

$$Q_{(1\text{-}2)} = \frac{Q_1 + Q_2}{2}$$

and

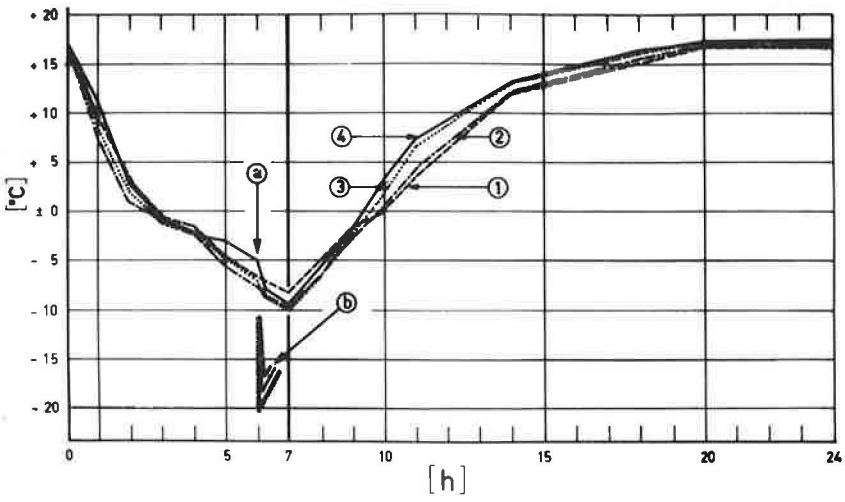

Figure 18. Temperature shock in concrete slabs in F-T-S test (1 = with 2-mm frozen water; 2 = alcohol; 3 = $CaCl_2$; 4 = NaCl; a = application time of de-icing agents 2, 3, and 4; b = reduction in surface temperature).

Figure 19. Comparison of chloride contents of concrete measured on roads in Switzerland and of test specimen.

Highway "Walenseestrasse„ :

Core taken just after Winter 1971

Original salt contents : Chloride contents in weight %

Core :	Nº 3 (Heavy F.S. - Damages)	0.11
	Nº 2 (Very heavy F.S. - Damages)	0.28
	Nº 4 (No F.S. - Damages)	0.10
	Nº 5 (No F.S. - Damages)	0.13

Highway "N13 GR Umfahrung Nufenen„:

Core taken in summer 1971
Panel 794 after 100 F.T.S. - cycles ($Ca Cl_2$) 0.08

Salt contents after F.T.S. test D-R : Chloride contents in weight %

Highway "N6 Bern - Spiez„ :

Core taken in summer 1972

Coro 1 b	after 500 F.T.S. - cycles ($Ca Cl_2$)	0.09
Coro 1 d	after 500 F.T.S. - cycles ($Ca Cl_2$)	0.10
Panel 221s	after 250 F.T.S. - cycles ($Ca Cl_2$)	0.15
" "	" " " (Na Cl)	0.12

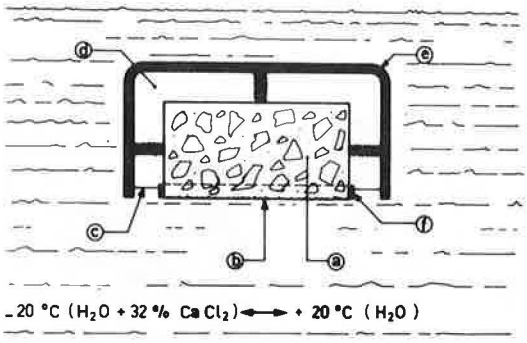

Figure 20. Schematic drawing of isolated F-T-S test specimen (a = specimen; b = pavement surface; c = water level; d = air; e = plastic box; f = insulation tape).

Figure 21. Schematic drawing of prism with eight measuring marks (a = concrete surface; b = measuring cone; c = mark fixed with epoxy).

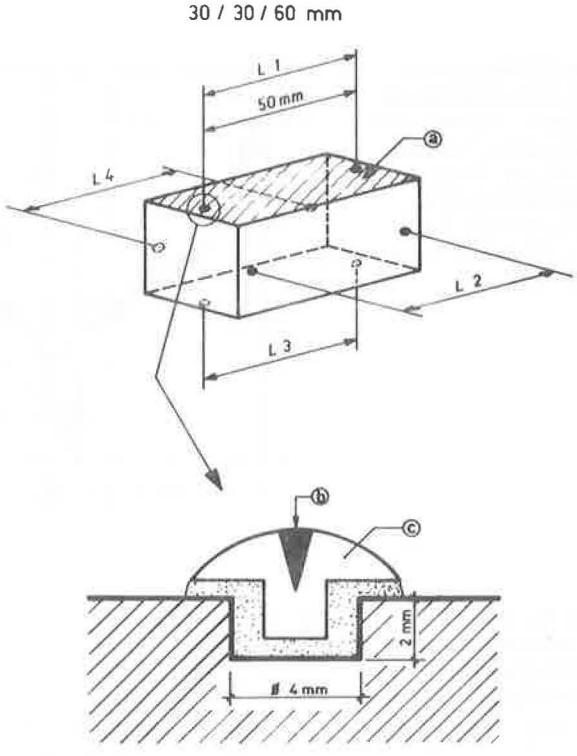

Figure 22. Cutting six prisms from a 28-day-old concrete slab core.

Figure 23. Fastening measuring marks to specimens.

Figure 24. Measuring axial length L.

Figure 25. Measuring transverse length of Q perpendicular to prism's axis.

$$Q_{(3-4)} = \frac{Q_3 + Q_4}{2}$$

In addition to the length changes, further measurements can be carried out by measuring the loss of the static modulus of elasticity. In this case, Young's modulus of elasticity for three additional prism specimens must be determined prior to the F-T-S test.

During and after the F-T-S test, additional moduli of elasticity (E_x) are determined on two test specimens from which an effective loss (in percent) in modulus of elasticity $\frac{\Delta E}{E}$ is computed. The static moduli of elasticity are measured by the same instruments and measuring marks as those used for length determination in the F-T-S test.

Evaluation of Measurements

Figures 26 and 27 show the results of axial expansion L and transverse expansion Q respectively of a tested concrete (No. 39). For evaluation of the linear expansion, the mean value of 24 axial and 24 transverse measurements are determined. Triaxial expansion M is determined from L, $Q_{(1-2)}$, and $Q_{(3-4)}$:

$$M = \frac{L + Q_{(1-2)} + Q_{(3-4)}}{3}$$

Figure 28 shows mean values of three measuring phases at 42, 154, and 395 cycles. Based on the mean value of L, the performance curves of F-T-S resistance for concrete No. 39 can be plotted (Fig. 28). Volumetric expansion V and the loss of weight can also be determined if required.

Relation Between Expansion and Loss in Modulus of Elasticity

The relation between length change and loss in modulus of elasticity is shown in Figures 29 and 30. Figure 29 shows the relation between the axial change in initial length and the loss (in percent) in modulus of elasticity $\frac{\Delta E}{E}$ experimentally obtained by Klieger in 1952. Figure 30 shows the relation between axial expansion triaxial expansion, volumetric expansion, and loss in modulus of elasticity. It is based on tests done by the authors. L represents the internal damage of the tested concrete; M and V represent its internal and external damage.

The authors believe that the number of experiments carried out to determine the relationship shown in Figure 30 for M and V is too limited.

Determination of Frost or F-T-S Resistance

The assessment is based on axial expansion and the corresponding number of cycles Z. Figure 31 shows the determination of F-T-S resistance. On the abscissa, L in percent of initial length and the loss (in percent) of modulus of elasticity $\frac{\Delta E}{E}$ are charted; on the ordinate the number of cycles is shown. The criterion for determination of F-T-S resistance is based on the relationship between the critical expansion L = 1 percent of the initial length, the number of cycles, and the durability factor. Expansion L = 1 percent of the initial length represents

1. ≥ 360 cycles—a high to very high F-T-S resistance (thickly hatched section of triangle AOB) corresponding to a durability factor > 80 percent,
2. 180 to 360 cycles—a medium F-T-S resistance (lightly hatched section of triangle BOC) corresponding to a durability factor = 80 to 50 percent, and
3. 180 cycles—a low to very low F-T-S resistance (plain section COD) corresponding to a durability factor ≤ 50 percent.

The dotted line is the performance curve of concrete No. 39 (Fig. 31). This concrete, at 395 cycles, expanded only 0.21 percent of the initial length and its F-T-S resistance should be rated high to very high. At 200 cycles no loss in modulus of elasticity

Figure 26. Results of axial expansion L (A = initial measurement; B, C, D = measurements after 42, 154, and 395 cycles; La, Lb, Lc, Ld, Le, Lf = specimens).

№ 39			42 Z			154 Z			395 Z		
		A	B	B–A ‰	‰	C	C–A ‰	‰	D	D–A ‰	‰
La	1	2449	2450	1		2452	3		2447	+2	
	2	2851	2852	1		2857	6		2866	15	
	3	2178	2180	2		2183	5		2185	7	
	4	2308	2306	0		2310	4		2320	14	
M/4 ‰				1	0,02		5	0,10		9	0,18
Lb	1	2457	2459	2		2463	6		2464	7	
	2	2779	2780	1		2783	4		2785	6	
	3	2737	2738	1		2741	4		2742	5	
	4	2571	2574	3		2577	6		2585	14	
M/4 ‰				2	0,04		5	0,10		8	0,16
Lc	1	2438	2440	2		2447	9		2447	9	
	2	2551	2553	2		2556	5		2560	9	
	3	2420	2422	2		2427	7		2429	9	
	4	2689	2690	1		2690	1		2692	3	
M/4 ‰				2	0,02		6	0,12		8	0,16
Ld	1	2687	2691	4		2698	11		2705	18	
	2	2502	2504	2		2509	7		2515	13	
	3	2351	2354	3		2357	6		2361	10	
	4	2605	2609	4		2613	8		2621	16	
M/4 ‰				3	0,06		8	0,16		14	0,28
Le	1	2529	2531	2		2537	8		2543	14	
	2	2515	2519	4		2524	9		2528	13	
	3	2499	2500	1		2504	5		2507	8	
	4	2591	2592	1		2595	4		2600	9	
M/4 ‰				2	0,04		7	0,14		11	0,22
Lf	1	2637	2638	1		2643	6		2647	10	
	2	2609	2612	3		2626	15		2690	81	
	3	2474	2476	2		2481	7		2510	36	
	4	2543	2548	3		2549	6		2555	12	
M/4 ‰				2	0,04		9	0,18		35	0,70
M ‰					0,04			0,13			0,28

Figure 27. Results of transverse expansion Q (A = initial measurement; B, C, D = measurements after 42, 154, and 395 cycles; Qa, Qb, Qc, Qd, Qe, Qf = specimens).

№ 39			42 Z			154 Z			395 Z		
		A	B	B–A ‰		C	C–A ‰		D	D–A ‰	
Qa	1	1548	1551	3		1560	12		1597	49	
	2	0922	0925	3		0938	16		0998	76	
	3	1005	1007	2		1015	10		1045	40	
	4	1311	1308	3		1317	6		1344	33	
M/4 ‰			Q 1/2 = 0,10	Q 3/4 = 0,00		Q 1/2 = 0,46	Q 3/4 = 0,26		Q 1/2 = 2,08	Q 3/4 = 1,22	
Qb	1	0520	0524	4		0543	23		0572	52	
	2	0900	0900	0		0920	20		0952	52	
	3	0822	0825	3		0835	13		0857	35	
	4	1551	1557	6		1567	16		1602	51	
M/4 ‰			Q 1/2 = 0,07	Q 3/4 = 0,17		Q 1/2 = 0,73	Q 3/4 = 0,50		Q 1/2 = 1,72	Q 3/4 = 1,42	
Qc	1	1068	1074	6		1086	18		1103	35	
	2	1114	1120	6		1133	19		1106	46	
	3	1656	1661	5		1675	19		1687	21	
	4	1936	1938	2		1948	12		1968	32	
M/4 ‰			Q 1/2 = 0,20	Q 3/4 = 0,13		Q 1/2 = 0,63	Q 3/4 = 0,53		Q 1/2 = 1,32	Q 3/4 = 0,89	
Qd	1	0904	0909	5		0923	19		0972	68	
	2	1396	1403	7		1412	16		1440	44	
	3	1690	1693	3		1701	11		1740	50	
	4	2231	2234	3		2245	14		2265	34	
M/4 ‰			Q 1/2 = 0,20	Q 3/4 = 0,10		Q 1/2 = 0,59	Q 3/4 = 0,43		Q 1/2 = 1,85	Q 3/4 = 1,39	
Qe	1	1457	1461	4		1470	13		1493	36	
	2	0673	0675	2		0683	10		0705	32	
	3	1362	1363	1		1381	19		1388	26	
	4	1528	1529	1		1536	8		1556	28	
M/4 ‰			Q 1/2 = 0,10	Q 3/4 = 0,03		Q 1/2 = 0,40	Q 3/4 = 0,45		Q 1/2 = 1,12	Q 3/4 = 0,89	
Qf	1	0850	0856	6		0868	18		0895	45	
	2	0638	0645	7		0660	22		0730	92	
	3	1098	1100	2		1109	11		1128	30	
	4	1850	1854	4		1865	15		1902	52	
M/4 ‰			Q 1/2 = 0,23	Q 3/4 = 0,10		Q 1/2 = 0,66	Q 3/4 = 0,43		Q 1/2 = 2,28	Q 3/4 = 1,35	
M ‰			0,15	0,09		0,58	0,43		1,73	1,19	

Figure 28. Mean values of L and M at 42, 154, and 395 cycles.

№ 39	Z	L ‰	Q 1/2 ‰	Q 3/4 ‰	M ‰
	42	0,04	0,15	0,08	0,09
	154	0,13	0,58	0,46	0,39
	395	0,21	1,77	1,21	1,06

Figure 29. Relation between axial expansion and loss elasticity.

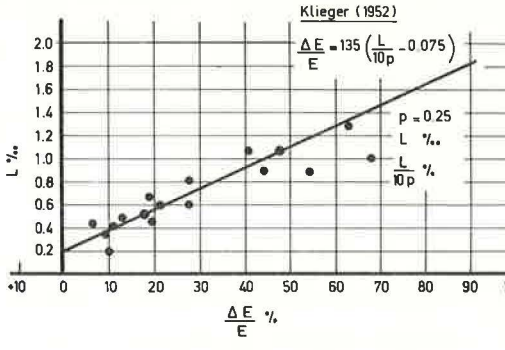

Figure 30. Relation between axial, triaxial, and volumetric expansion and the loss in modulus of elasticity.

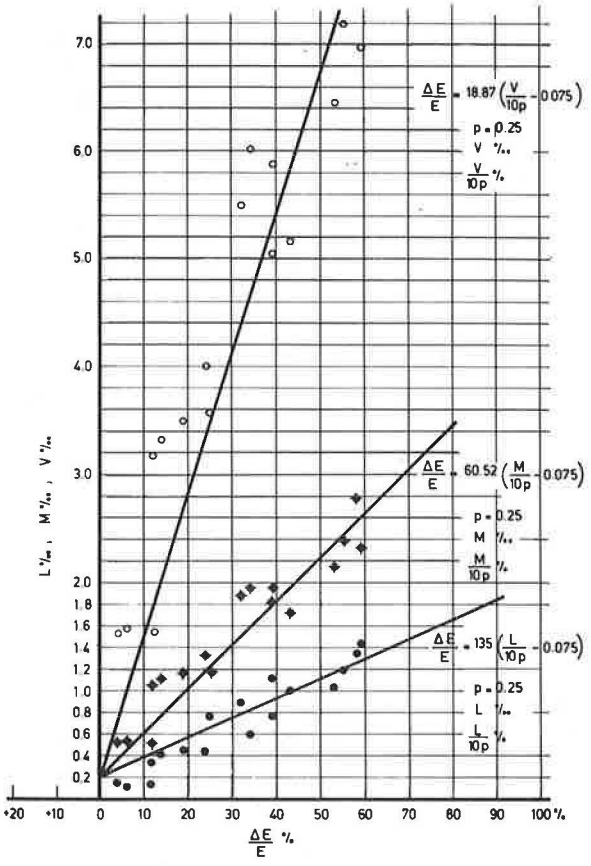

Figure 31. Determination of F-T-S resistance.

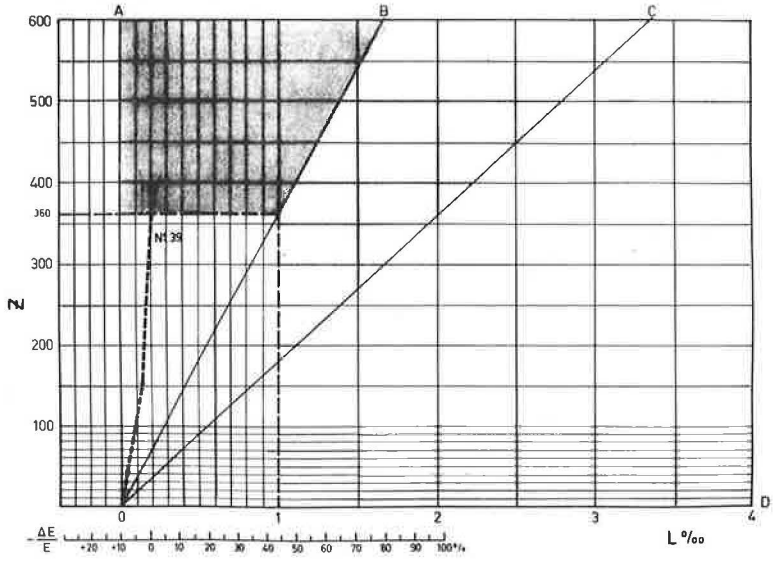

$\left(\frac{\Delta E}{E} + 1 \text{ percent of the initial length}\right)$ occurs. The durability factor is therefore equal to 101 percent and the quality of concrete No. 39 should be rated very high.

During concrete road construction this test is used only as a checking control method and is applied when F-T-S resistance, resulting from characteristic values, is medium, low, or very low or when the morphological examination of the concrete shows a disturbance factor ≥ -10.

PRACTICAL INVESTIGATION PROCEDURE

Tests are carried out prior to and during construction. Prior to construction a first examination is done on laboratory-prepared specimens. Approximately 10 to 14 days before construction, additional trial-run tests are occasionally performed on a trial section.

Initial Laboratory Tests

Tests take place a few months before construction is begun to obtain a concrete with optimum properties from the available materials or to change the mix design to achieve an optimal solution.

Concretes are produced with specified aggregate and cement type and composition, as follows:

1. Water-cement ratio (0.4 to 0.45 or 0.5),
2. Cement content (350 to 400 kg/m^3),
3. Air-entraining agent (compared to parallel examination with Vinsol Standard), and
4. Air-entraining agent dose (1.0 to 1.5 or 1.7 percent).

The test is carried out on concrete prisms 12 by 12 by 36 cm.

Examined quantities are total air content of fresh concrete, concrete workability with VEBE apparatus, dry and wet densities of concrete, flexural strength at 28 days, compressive strength at 28 days, and elastic modulus at 28 days. One prism is reserved for

1. Microscopic, pore analytical determination of the F-T-S resistance,
2. Microscopic, morphological examination of the concrete, and
3. F-T-S test (D-R) with rapid frost cycles.

Test results make it possible to specify the type and dose of the air-entraining agent and cement content. They also indicate the suitability of the aggregate and its grading. Controlling values for assessment are F-T-S resistance and morphological quality determinations and concrete strengths.

Trial-Run Testing

The trial section of the pavement is laid 10 to 14 days before construction is begun. The performance of the batching plant and placing machinery and the accuracy of the measuring devices are checked. The concrete is mixed with the batched materials according to the mix designed after the laboratory tests, and one or more slab lengths are placed. After 1 or 2 days test cores of 15-cm diameter are bored from the trial slab, the remainder of which is broken up and removed.

The following controls are determined at batching: air content (Lf), workability, water-cement ratio, dose of air-entraining agent, and volume control of one mix in the compacted state. For the strength tests, prisms 12 by 12 by 36 cm are produced.

The following tests are carried out on the cores: (a) pore analysis and determination of F-T-S resistance from characteristic values, (b) morphological quality assessment of the concrete, and (c) F-T-S test.

A comparison of these results with those of the initial laboratory tests makes quality control of the concrete and determination of deviations and their causes and, under some circumstances, the implementation of improvement measures possible.

Investigations During Construction

During the first few days of construction, cores in sufficient numbers for two or three tests are taken daily from critical positions, such as places with drier or wetter concrete or where there were disturbances during paving.

The initial test results are telephoned to the site, and the amount of subsequent boring depends on these results. A minimum of one test per 2500 m^2 is specified. Test results pertaining to Highway N1/St. Gallen-Buriet are shown in Figure 32. This highway section is 8.5 km long and was constructed in 1972. The concrete pavement construction costs amounted to Fr. 5.4 million, and the testing costs to Fr. 24,000.

In Figure 32, the initial test results indicate a pronounced variation in total air content of fresh concrete (col. 6) and of hardened concrete (col. 9). In certain cases a high proportion of large pores(> 0.3-mm diameter) and a relatively high water intake A_5 (col. 15) from 12 to 14 percent in volume were evident. (Normal is a water intake of 10 to 12 percent in volume.)

As a first step, the conveyor belt on which the concrete was forwarded from the truck to the distribution hopper was removed. Simultaneously a thorough control of the batching plant and the aggregate was done, which showed that the aggregate fines proportion (< 0.2 mm) in the concrete was too high and was not in accordance with the standard specifications. With most of the aggregate delivered, the improvements could only be brought about gradually. An improvement in the test results is detectable from slab 1310 to slab 2759. The high water intake and the decreased workability as well as the too high content of large pores could possibly be caused by the high proportion of fines. Results of the F-T-S test (cols. 25 to 28) show that, in this specific case, the high fines proportion did not affect F-T-S resistance.

CORRELATION BETWEEN PRINCIPLES

From tests performed on 69 old and new concretes, the documented correlation was made. The results are shown in Figure 33 and include

1. Characteristic values with pore analytical determination of the F-T-S resistance (cols. 8 to 19),
2. Morphological quality assessment of the concretes (col. 20), and
3. F-T-S test results from the D-R method (cols. 21 to 25).

D-R test results are shown in Figures 34 through 37. The correlation between principles can be established by a comparison of F-T-S resistances and those determined from characteristic values. The influence of morphological quality assessment of the tested concrete on the F-T-S resistance is shown in Figures 34 and 35.

Figure 34 shows concretes that have a high or very high resistance based on characteristic values (cols. 8 to 19 of Fig. 33) and that have a disturbance factor < -10 (col. 20).

All concretes except Nos. 31, 43, 45, 48, and 49 lie within triangle AOB and indicate high to very high F-T-S resistance. This illustration shows a very good correlation between the two methods (D-R and characteristic values).

Figure 35 similarly shows concretes that, from their characteristic values, indicate a high to very high F-T-S resistance but have considerably greater disturbance factors ($\geq$ -10). Of the 12 concretes only 5 lie inside triangle AOB indicating a high to very high resistance. Of the remaining seven, four lie in the medium resistance zone (triangle BOC), and three are inside triangle COD denoting a low to very low F-T-S resistance. Figure 35 proves that a disturbance factor of $\geq$ -10 may jeopardize F-T-S resistance assessed by means of pore analysis.

Figure 36 shows concretes that have a medium F-T-S resistance according to their characteristic values and a disturbance factor of -5 to -16. The number of concretes within the medium F-T-S resistance range was relatively low, and poor correlation must be improved by further investigations.

Figure 37 shows concretes with low or very low F-T-S resistance, according to their characteristic values, with disturbance factors between -7 and -13. As a result of the D-R test, all investigated concretes range within the triangle COD for low to very low F-T-S resistance, which gives a complete correlation.

Figure 32. Test results of Highway N1/St. Gallen-Buriet.

1	2	3	4	5	6	7	8	9	10	11	12	13	14	15	16	17	18	19	20	21
					Concrete characteristics			Pore analysis - f t s - resistance												
Slab Nr	Date of Concreting	Nr. LPM	Received by LPM	LPM Report	Air-voids	VE-BE	W/C	"La"	L300	"R"	"α"	"AF"	"P_i"	"A_5"	"A_V"	"V"		"WB"		Evaluation According Columns
					%	sec	Ratio	Vol%	Vol%	mm^{-1}	mm	mm	Ratio	Vol%	Vol%	V_1	V_2	WB_1 kg/cm²	WB_2 kg/cm²	9 - 20
27084	5.7.72	A243	20.7.72	4.8.72	4,0	14,5	0,40	7,54	3,39	0,082	73,1	0,046	259	10,7	15,5	61,6	31,6	5022	2592	very high
27085	"	"	"	"	5,2	6,0	0,45	6,27	3,25	0,088	68,1	0,063	176	11,2	18,3	54,1	29,0	3650	1960	hig-v high
27086	"	"	"	"	4,9	8,0	0,40	5,43	2,86	0,083	71,4	0,067	180	11,7	16,1	44,0	24,4	3560	2025	high
27083	"	"	"	"	4,0	17,0	0,40	-	-	-	-	-	-	-	-	-	-	-	-	"
2	21.8.72	L-298	28.8.72	15.9.72	7,3	6,2	0,43	6,29	4,15	0,093	65,2	0,064	153	12,2	16,4	59,2	34,0	3540	2040	very high
7	"	L-299	"	"	3,2	16,0	0,43	2,50	1,49	0,086	69,7	0,093	74	11,5	15,3	23,6	12,9	1440	780	medium
14	"	L300	"	"	7,7	-	-	11,29	5,21	0,160	37,5	0,662	51	8,8	11,3	144,7	59,2	8640	3540	very high
16	22.8.72	L-301	"	"	5,1	-	-	6,05	3,20	0,089	66,6	0,066	166	12,6	17,1	43,3	25,4	2580	1500	high
23	"	L-302	"	"	4,0	16,0	0,37	6,81	2,81	0,088	68,1	0,058	187	11,8	17,4	42,5	23,8	2580	1440	"
39	24.8.72	L-303	"	"	5,0	9,0	0,46	5,96	3,79	0,087	69,7	0,063	177	11,3	16,4	62,1	33,5	3720	2040	very high
62	"	L-304	"	"	5,8	10,0	0,43	18,87	2,01	0,220	27,2	0,051	34	12,4	16,1	27,9	16,2	1680	960	medium
85	25.8.72	L-305	"	"	11,5	-	-	8,30	1,02	0,178	33,7	0,097	29	12,4	18,0	14,0	8,1	840	480	"
89	"	L-306	"	"	11,0	-	-	9,29	1,95	0,149	40,0	0,072	54	12,3	18,6	27,4	15,8	1620	960	medium-high
90	"	L-307	"	"	7,0	-	-	7,19	1,64	0,143	41,6	0,090	47	11,9	19,0	24,4	13,7	1440	840	medium
110	28.8.72	L-309	29.8.72	2.10.72	9,0	10,0	0,45	5,46	2,18	0,112	53,9	0,085	76	12,8	17,6	28,6	17,0	1716	1020	high
145	29.8.72	L-310	"	"	6,0	9,0	-	11,33	2,73	0,156	38,4	0,062	57	13,2	19,6	34,1	20,6	2046	1236	"
210	30.8.72	L-311	"	"	6,0	-	-	5,79	3,37	0,096	62,5	0,072	125	12,8	20,4	44,3	26,3	2658	1578	"
219	"	L-312	"	"	4,4	-	-	11,55	3,23	0,124	48,4	0,048	116	13,7	20,2	38,0	23,5	2280	1410	"
247	1.9.72	L-313	"	"	12,0	14,0	0,37	7,04	1,56	0,128	46,9	0,076	64	13,3	18,9	19,2	11,7	1152	702	medium
302	4.9.72	L-314	"	"	7,0	-	-	6,94	2,17	0,126	47,4	0,082	65	13,0	17,4	27,8	16,6	1668	996	"
350	5.9.72	L-315	"	"	12,1	-	-	11,61	1,51	0,176	34,2	0,068	41	14,0	18,9	17,1	10,7	1026	642	"
372	"	L-316	"	"	10,5	-	-	9,94	2,26	0,134	44,8	0,061	79	13,1	20,0	28,6	17,2	1716	1032	high
450	7.9.72	L-317	14.9.72	18.9.72	5,8	-	-	8,02	3,32	0,088	68,4	0,049	228	13,5	19,2	40,0	24,5	2400	1500	"
462	"	L-318	"	"	11,0	16,0	0,45	6,91	3,01	0,096	62,3	0,063	148	13,6	19,2	35,8	22,1	2148	1320	"
510	8.9.72	L-319	"	"	9,5	-	-	7,78	3,16	0,116	53,2	0,065	104	12,5	19,1	43,2	25,3	2592	1518	"
612	12.9.72	L-320	"	"	-	-	-	13,53	3,03	0,150	40,0	0,050	77	12,9	19,7	39,3	23,4	2358	1404	"
614	"	L-321	"	"	4,2	-	-	8,66	3,43	0,108	55,3	0,056	129	13,4	19,8	41,8	25,5	2508	1530	"
M1-3	"	L-322	"	"	-	-	-	7,06	2,51	0,120	50,3	0,076	79	11,8	18,3	38,0	21,2	2280	1260	"
B4-6	"	L-323	"	"	4,8	-	-	4,93	2,76	0,092	65,2	0,074	121	12,2	19,0	39,4	22,6	2364	1356	"
634	18.9.72	L-324	20.9.72	22.9.72	5,9	6,2	0,42	7,11	1,75	0,124	48,0	0,076	70	14,0	20,8	19,8	12,5	1188	750	medium
622	"	L-325	"	"	12,3	-	0,45	5,72	2,05	0,112	53,2	0,085	76	13,5	20,4	24,6	15,1	1476	906	medium-high
686	19.9.72	L-326	4.10.72	23.10.72	6,0	10,5	0,37	5,75	3,30	0,100	59,8	0,070	109	12,8	17,8	43,4	25,7	2604	1542	high
760	20.9.72	L-327	"	"	4,1	10,0	0,42	7,48	3,08	0,110	55,0	0,063	110	13,6	19,9	36,6	22,6	2196	1356	"
819	21.9.72	L-328	"	"	7,0	8,0	0,41	7,36	3,11	0,096	61,9	0,056	155	13,4	19,4	37,9	23,2	2274	1392	"
943	25.9.72	L-329	"	"	5,8	7,5	0,43	8,91	2,28	0,120	50,1	0,059	99	12,9	19,7	29,6	17,6	1776	1056	"
982	26.9.72	L-330	"	"	5,8	8,0	0,40	6,87	2,98	0,106	56,8	0,065	112	13,8	19,3	34,6	21,5	2076	1290	"
1004	27.9.72	L-331	"	"	5,2	10,0	0,39	7,94	2,87	0,098	60,8	0,052	158	13,6	20,1	34,1	21,1	2046	1266	"
1036	28.9.72	L-332	"	"	7,8	12,0	0,40	5,16	1,60	0,120	50,4	0,091	58	13,0	18,7	20,5	12,3	1230	738	medium
1093	29.9.72	L-333	27.10.72	13.11.72	7,5	13,0	0,39	5,67	3,18	0,102	58,4	0,075	100	12,5	19,2	43,5	25,4	2610	1524	high
1190	2.10.72	L-334	"	"	6,0	10,0	0,37	6,26	2,11	0,114	52,7	0,073	81	13,1	19,2	26,7	16,1	1602	966	medium-high
1310	9.10.72	L-335	"	"	4,8	13,0	0,38	7,00	2,77	0,100	59,6	0,061	131	12,8	18,5	36,4	21,6	2184	1296	high
1434	11.10.72	L-336	"	"	4,8	8,0	0,43	5,26	2,90	0,102	59,1	0,078	96	13,0	19,5	37,1	22,3	2226	1338	"
1566	13.10.72	L-337	"	"	5,4	9,0	0,43	8,07	4,16	0,104	58,1	0,056	140	13,2	21,0	52,0	31,5	3120	1890	high-v high
1679	16.10.72	L-338	"	"	6,5	10,0	0,46	5,76	2,93	0,106	56,9	0,080	94	12,5	20,0	40,1	23,4	2406	1404	high
1836	19.10.72	L-339	"	"	8,0	9,0	0,43	7,89	3,93	0,096	62,2	0,054	168	12,9	20,1	51,0	30,4	3060	1824	high-v high
1983	25.10.72	L-340	31.10.72	20.12.72	6,0	6,0	0,45	7,28	4,71	0,116	52,0	0,071	91	11,9	19,5	70,2	39,5	4212	2370	very high
2097	31.10.72	L-341	"	"	5,4	11,0	0,43	8,78	4,77	0,100	60,1	0,050	168	11,8	17,8	72,2	40,4	4332	2424	" "
2281	3.11.72	L-342	"	"	6,2	10,5	0,43	7,90	3,76	0,118	50,5	0,066	90	11,3	18,2	61,9	33,4	3714	2004	" "
2424	7.11.72	L-343	"	"	5,2	10,0	0,41	6,68	3,44	0,108	55,8	0,069	103	11,6	18,5	53,7	29,6	3222	1776	high-v high
2557	10.11.72	L-344	"	"	4,5	10,0	0,40	5,90	2,71	0,106	56,9	0,075	97	12,6	18,7	36,6	21,5	2196	1290	high
2710	15.11.72	L-345	"	"	4,2	11,0	0,40	7,99	3,99	0,116	51,8	0,061	98	11,7	19,8	61,3	34,1	3678	2046	very high
2729	"	L-346	"	"	4,5	10,0	0,41	8,04	4,37	0,104	57,8	0,055	138	11,8	18,8	66,2	37,0	3972	2220	" "
2759	17.11.72	L-348	"	"	4,5	8,5	0,41	11,46	5,88	0,112	53,2	0,042	153	11,6	20,4	91,8	50,6	5508	3036	" "

Tabell 6 Test Results Highway N1 / St Gallen - Buriet (Nr 27'083 - 27'086 = Laboratory Test Results)

Figure 32. Continued.

22	23	24	25				26				27				28			
Morpho-logical evaluation	Remarks		Frost - Thawsalt - Resistance Test Results (Method D - R)															
Distur-bance Factor	Site Rating + and -	Carrots	Expansion L, Q, M ‰															
			Nr of Cycles Z	L ‰	Q ‰	M ‰	Z	L ‰	Q ‰	M ‰	Z	L ‰	Q ‰	M ‰	Z	L ‰	Q ‰	M ‰
-9	keine	5.7.72	50	0,11	0,08	0,10	150	0,52	1,00	0,76	330	1,69	3,97	2,83	-	-	-	-
-7	keine	"	50	0,17	0,28	0,23	150	0,46	0,88	0,67	330	1,40	2,89	2,15	-	-	-	-
-7	keine	"	50	0,08	0,14	0,11	150	0,39	0 84	0,62	330	0,98	2,28	1,63	-	-	-	-
-	keine	"	50	0,12	0,22	0,17	150	0,28	0,79	0,54	330	0,61	1,83	1,22	-	-	-	-
-6	-	9.10.72	50	0,10	0,23	0,19	150	0,12	0,62	0,45	300	0,30	1,60	1,17	500	0,63	3,30	2,41
-7	-	9.10.72	50	0,10	0,19	0,16	150	0,18	0,73	0,58	300	1,09	2,73	2,15	400	1,86	5,46	4,26
-16	-	9.10.72	50	0,12	0,17	0,15	150	0,54	0,72	0,66	300	1,38	1,67	1,57	400	2,10	2,63	2,45
-7	+	-																
-4	-	-																
-5	+	9.10.72	50	0,04	0,13	0,10	150	0,13	0,51	0,38	300	0,20	1,04	0,76	500	0,36	2,10	1,52
-12	+	9.10.72	50	0,07	0,17	0,14	150	0,17	0,64	0,48	300	0,53	1,72	1,32	400	0,68	2,63	1,98
-9	-	9.10.72	100	0,12	0,47	0,35	200	0,23	1,05	0,78	300	0,45	1,77	1,33	400	0,82	2,90	2,21
-10	-	-																
-7	-	-																
-7	-	-																
-12	+	-																
-15	+	-																
-9	+	-																
-12	-	9.10.72	100	0,13	0,54	0,40	200	0,30	1,41	1,04	300	0,49	2,36	1,74	400	0,71	4,33	3,12
-7	-	9.10.72	100	0,13	0,40	0,31	200	0,31	0,91	0,71	300	0,46	1,80	1,35	400	0,74	3,17	2,36
-16	-	9.10.72	100	0,11	0,54	0,40	200	0,26	1,32	0,97	300	0,62	3,22	2,35	400	0,80	5,24	3,76
-7	-	-																
-8	+	-																
-11	-	-																
-16	-	-																
-16	-	9.10.72	100	0,11	0,47	0,35	200	0,27	1,16	0,86	300	0,49	2,59	1,89	400	1,19	4,87	3,64
-6	+	-																
-7	+	-																
-4	+	-																
-12	+	9.10.72	100	0,08	0,45	0,33	200	0,28	1,12	0,84	300	0,51	2,06	1,54	400	1,03	4,02	3,02
-8	+	17.1.73	50	0,05	0,12	0,10	200	0,07	0,27	0,20	370	0,17	0,73	0,54				
-6	-																	
-5	-																	
-7	+																	
-12	+	17.1.73	50	0,06	0,14	0,11	200	0,13	0,37	0,29	370	0,35	1,91	1,39				
-11	+																	
-14	+																	
-7	-	17.1.73	50	0,04	0,08	0,07	200	0,12	0,43	0,32	370	0,19	1,64	1,16				
-7	-																	
-5	+	17.1.73	50	0,08	0,11	0,10	200	0,17	0,29	0,25	370	0,36	2,10	1,52				
-9	-																	
-5	-																	
-9	+	17.1.73	50	0,05	0,04	0,04	200	0,09	0,16	0,13	370	0,16	0,50	0,39				
-6	-																	
-3	+																	
-2	-																	
-3	+	22.12.72	50	0,09	0,28	0,21	200	0,14	0,83	0,60	370	0,34	2,14	1,54				
-2	+																	
-2	+																	
-8	-																	
-3	-	22.12.72	50	0,08	0,20	0,16	200	0,13	0,99	0,71	370	0,09	2,19	1,49				
-4	-	22.12.72	50	0,09	0,24	0,19	200	0,15	0,81	0,59	370	0,26	1,52	1,10				
-6	-	22.12.72	50	0,06	0,19	0,15	200	0,18	1,21	0,87	370	0,09	2,12	1,45				

Figure 33. Test results of 69 concretes.

1	2	3	4	5	6	7	8	9	10	11	12	13	14	15	16	17	18	19
Con-crete		LPM	Concrete charateristics				Pore analysis - f t s - resistance											
Nr.	Provenience	Serial Nr	W/C	VEBE sec	Flecturall Strength kg/cm²	Air Contents %	L %	L 300 %	α	Pi	AF mm	A_5 %	Av %	V_1	V_2	WB_1 kg/cm²	WB_2 kg/cm²	Previsions According 8 - 18
1	Sursee	A-179 E	0 40	—	—	4.9	6 191	2 771	54 5	89 4	0 075	11 0	16 3	47 7	25 1	2862	1508	high very high
2	N1 St Gallen (Feld 39)	L 303	0 46	9 0	—	5 0	5 958	3 789	69 7	177 0	0 063	11 3	18 4	62 1	33 0	3720	2040	high
3	Bordstein _ Elementbeton	A-251	0 48	—	—	4 4	4 64	3 05	83 9	242 2	0 060	14 3	19 8	33 5	21 3	2010	1278	"
4	N6 Kiesen _ Spiez	F/11 / A	—	—	—	4 0	6 407	2 051	52 6	84 1	0 075	10 3	14 3	40 1	19 9	3008	1493	"
5	" "	"	—	—	—	"	"	"	"	"	"	"	"	"	"	"	"	"
6	" "	"	—	—	—	"	"	"	"	"	"	"	"	"	"	"	"	"
7	" "	"	—	—	—	"	"	"	"	"	"	"	"	"	"	"	"	"
8	" "	"	—	—	—	"	"	"	"	"	"	"	"	"	"	"	"	"
9	" "	"	—	—	—	"	"	"	"	"	"	"	"	"	"	"	"	"
10	N 12 Landquart	A 225	0 45	8 0	62 7	3 6	3 361	1 617	71 4	106 7	0 086	12 0	17 9	28 4	13 5	1780	846	"
11	N 6 Kiesen _ Spiez	F/ 11/A	—	—	—	—	6 407	2 051	52 6	84 1	0 075	10 3	14 3	40 1	19 9	3008	1493	"
12	N 13 Landquart	A 225	0 45	7 0	76.0	3.2	5 204	1 891	61.8	122 3	0 074	10 5	15 0	35 6	18 0	2705	1368	"
13	N 6 Kiesen (Restplatz)	A 191	0 42	—	—	5 0	4 327	1 033	61.0	85 9	0 080	9 2	12 8	47 2	22 0	2820	1320	medium
14	Sursee	A-179 E	0 40	—	—	4 4	4 266	1 075	46 8	40 1	0 107	11 4	15 1	17 4	9 4	1044	564	"
15	Sursee	A-179 E	0 42	8 0	—	4 0	4 154	1 359	52 6	54 6	0 100	12 1	16 9	19 7	11 2	1182	720	very high
16	N1 St Gallen (Feld 2)	L-298	0 43	6 2	—	7.3	6 287	4 146	65 2	153 0	0 064	12 2	16 4	59 2	34 0	3540	2040	"
17	Lixibach	A-207	0 40	7 0	61 5	4.5	6 853	5.140	91.0	456 6	0 041	11 3	15 2	84 2	45 5	5178	2798	"
18	Tessin	A-168 E	0 40	9 0	66 2	2.7	4 584	2 984	73 1	161 9	0 066	9 9	13 0	63 4	30 1	4197	1993	medium
19	N1 St Gallen (Feld 85)	L 305	—	—	—	11 5	8 299	1 016	33 7	29 0	0 097	12 4	18 0	14 0	8 1	840	480	"
20	N1 St Gallen (Feld 350)	L 315	—	—	—	12.1	11 610	1 510	34.2	41 0	0 068	14 0	18 9	17.1	10 7	1026	642	very high
21	Sika AG	A-240	—	—	—	—	6 087	3 931	78.9	241 8	0 057	10 9	15.7	66.6	36 1	3996	2166	high v high
22	Tessin	A-239	0 40	11 0	70 2	3 4	5 386	3 263	75 0	211 6	0 064	11 5	17 5	59 2	28 3	4156	1987	high
23	N1 St Gallen (Feld 612)	L 320	—	—	—	—	13 53	3 03	400	77 0	0 050	12 9	19.7	39 3	23 4	2658	1404	high v high
24	N 13 Landquart	A-225	0 45	4 0	63 9	4 6	5 288	2 703	68.1	146 4	0 068	10 2	17 2	54 0	26 5	3451	1698	very high
25	N13 Landquart	A-225	0 50	6 0	63 6	4 2	7 358	3 930	61 8	168 3	0 080	11 9	18 0	58 6	33 0	3727	2099	high
26	Tessin	A-239	0 40	11 5	65.7	2.9	3 849	1 829	62.5	82 3	0 085	10 0	—	38 1	18 3	2503	1202	"
27	Tessin	A-239	0 45	4 5	55 5	5 0	5 726	2 569	57 6	99 0	0 083	12 7	17 2	38 3	20 2	2125	1121	medium
28	N1 St Gallen (Feld 62)	A-304	0 43	10 0	—	5 8	18 871	2 005	27 2	34 0	0 051	12 4	16 1	27 9	16 2	1680	960	"
29	N1 St Gallen (Feld 534)	L 324	0 43	6 2	—	5.9	7 110	1 750	47.9	70 0	0 076	14 0	20 8	19 8	12 5	1188	750	high
30	N 3 Rheinfelden	A-201	—	—	—	—	4 574	3 206	68 0	128 2	0 073	12 5	16 0	43 9	25 6	2290	1300	"
31	Gotthard 1971 (Feld 4a)	A-187 E	0.43	13 5	60 0	4.5	7 352	2 069	55 5	112 8	0 064	10 8	16.1	36 9	19 1	2220	1140	very high
32	Sika AG	A-240	—	—	—	—	6 683	4 123	63 8	151 4	0 053	10 7	16 6	72 2	39 5	4332	2316	medium
33	N1 St Gallen (Feld 247)	L 313	0 37	14 0	—	12 0	7 040	1 560	46 9	64 0	0 076	13 3	18 9	19 2	11 7	1152	702	"
34	N1 St Gallen (Feld 302)	L 314	—	—	—	7 0	6 940	2 170	47 4	65 0	0 082	13 0	17 4	27 8	16 6	1668	996	"
35	N3 Rheinfelden	A-175	0 42	—	70 0	—	4 621	1 645	54 5	64 3	0 087	12 7	15 3	22 0	12 9	1540	903	high
36	Tessin	A-168	0 40	11 5	65 7	2 9	3 849	1 829	62 5	82 3	0 085	—	—	38 1	18 3	2503	1202	"
37	N 13 Landquart	A-225	0 50	3.0	53 7	5 0	7 395	2 641	50 8	84 8	0 071	10 4	19 2	50 8	25 4	2728	1364	"
38	Tessin	A-168	0 45	8.0	58 6	4 0	5 309	2 187	61 2	111 4	0 076	10 6	15 2	40 5	20 6	2373	1207	"
39	Tessin	A-239	0 45	5 8	54 8	7 5	6 277	2 260	49 2	89 0	0 087	10 0	—	38 9	20 5	2132	1123	"
40	N 13 Landquart	A-225	0 45	5 0	54 7	4 4	6 317	2 237	58 8	112 3	0 079	11 6	19 1	36 6	18 7	2002	913	medium-high
41	Gotthard 1971 (Feld 1a)	A-186 E	0.43	16 0	60 0	3 9	6 397	1 543	47.6	63 4	0 086	12 2	18 0	22 0	12 6	1320	780	high
42	Tessin	A-168	0 45	5 8	54 8	7 5	6 277	2 260	49 2	89 0	0 087	—	—	38 9	20 5	2132	1123	"
43	Tessin	A-168	0 40	6 2	80 7	4 8	3 953	2 012	66 6	108 8	0 078	—	—	41 9	20 1	3381	1622	very high
44	Lixibach	A-207	0 45	4 0	57 5	5 7	5 415	3 864	88 5	325 1	0 052	11 5	19 0	61 2	33 6	3519	1932	high
45	N1 St Gallen	A-243	0 40	8 0	—	4 9	5 433	2 856	71 4	180 0	0 067	11 7	16 1	44 0	24 4	3560	2025	high-v high
46	Tessin	A-239	0 40	5 8	48 1	4 6	6 234	3 333	71 4	205 3	0 063	10 5	15 3	74 0	31 7	3559	1525	medium
47	N1 St Gallen (Feld 7)	L 299	0 43	16 0	—	3 2	2 494	1 480	69 7	74 0	0 093	11 5	15 3	23 6	12 9	1440	780	high
48	N 3 Rheinfelden	A-201	—	—	—	—	5 111	3 380	70 0	159 3	0 067	12 2	16 3	56 3	27 7	2800	1400	high-v high
49	N1 St Gallen	A-243	0 45	6 0	—	5 2	6 265	3 252	68 1	176 0	0 063	11 2	18 3	54 1	29 0	3650	1960	very high
50	N1 St Gallen	A-243	0 40	14 5	—	4 0	7 543	3 392	93 1	256 0	0 046	10 7	15 5	61 6	31 6	5022	2592	medium
51	N3 Rheinfelden	A-201	0 42	—	50 0	—	5 426	1 918	46 0	46 1	0 098	11 2	15 2	32 0	17 1	1600	850	very high
52	N1 St Gallen (Feld 16)	L 300	—	—	—	7 7	11 292	5 214	37 5	51 0	0 062	8 8	11 3	144 7	59 2	8640	3540	high-v high
53	Tessin	A-239	0 45	5 0	55 9	4 3	5 332	3 403	73 1	188 7	0 064	11 2	18 10	56 6	30 3	3164	1694	high
54	Tessin	A-168	0 45	4 5	59 4	8 5	5 985	2 510	57 6	101 2	0 077	—	—	43 2	22 8	2566	1354	"
55	Sika AG	A-240	—	—	—	—	6 441	3126	51 7	80 0	0 087	11 4	17 9	48 8	27 4	2928	1644	"
56	Tessin	A-239	0 45	3 0	52 7	7 0	5 241	2 350	53 5	72 7	0 093	11 1	19 5	46 0	21 2	2424	1117	medium
57	N3 Rheinfelden	A-175	—	—	—	—	4 661	1 946	46 8	43 5	0 104	10 8	—	34 8	18 0	2450	1260	low
58	N3 Rheinfelden	A-176	—	—	—	—	1 495	0 370	38 4	7 5	0 210	11 6	—	5 8	3 2	406	224	very low
59	N3 Rheinfelden	A-176	—	—	—	—	1 206	0 035	27 2	2 2	0 325	11 9	—	0 5	0 3	35	21	"
60	N6 Kiesen _ Spiez	A-191	—	—	—	6 8	1 741	0 278	34 0	5 7	0 224	10 1	12 3	5 7	2 8	360	180	medium
61	Bordsteine _ Elementbeton	A-251	0 43	—	—	4 8	2 643	1 353	62 5	55 9	0 101	12 4	14 5	18 7	10 9	1140	660	low
62	N6 Kiesen _ Spiez	F/ 11/ E	—	—	—	4 0	3 396	0 590	32 3	10 3	0 174	10 5	12 7	10 7	5 5	660	360	"
63	" "	"	—	—	—	"	"	"	"	"	"	"	"	"	"	"		"
64	" "	"	—	—	—	"	"	"	"	"	"	"	"	"	"	"		"
65	" "	"	—	—	—	"	"	"	"	"	"	"	"	"	"	"	"	very low
66	N3 Rheinfelden	A-176	—	—	—	—	1 468	0 088	26 0	2 3	0 312	12 8	—	1 2	0 7	84	49	low
67	N1 Lenzburg	A-205	—	—	—	—	3 193	0 628	37 0	15 1	0 154	7 9	10 7	23 3	7 9	1150	400	"
68	N6 Kiesen _ Spiez	F/ 11/ E	—	—	—	—	3 396	0 590	32 3	10 3	0 174	10 5	12 7	10 7	5 5	660	360	"
69	Hongrin	A-209	0 42	—	—	—	3 062	0 563	31 9	9 1	0 185	13 4	14 5	6 9	4 2	414	252	

Figure 33. Continued.

20	21				22				23				24				25			
Morpho - logical Evaluation	Frost - Thawsalt Resistance Test Results (Method D-R)																			
	Nr of Cycles Z	L °/oo	M °/oo	V °/oo	Z	L °/oo	M °/oo	V °/oo	Z	L °/oo	M °/oo	V °/oo	Z	L °/oo	M °/oo	V °/oo	Z	L °/oo	M °/oo	V °/oo
_6	100	0 04	0 25	0 77	200	0 08	0 52	1 57	400	0 12	1 01	3 03								
_5	42	0 04	0 10	0 30	154	0 13	0 38	1 15	300	0 20	0 76	2 28	395	0 21	1 06	3.19	500	0 36	1 52	4 56
_5	50	0 00	0 09	0 18	160	0 11	0 09	0 27	306	0 16	0 17	0 50	465	0 29	0 19	0 57				
_6	50	0 03	0 29	0 89	200	0 14	0 51	1 55	400	0 26	1 54	4 62								
"	50	0 05	0 09	0 26	200	0 14	0 67	2 00	390	0 33	1 85	5 56								
"	50	0 07	0 08	0 23	200	0 12	0 53	1 59	390	0 35	1 78	6 35								
"	50	0 06	0 07	0 20	200	0 14	0 68	2 05	390	0 85	1 89	5 68								
"	50	0 03	0 25	0 75	200	0 17	0 47	1 42	400	0 35	1 07	3 20								
"	50	0 09	0 23	0 70	250	0 19	1 06	3 20	500	0 61	2 30	6 90								
_3	50	0 05	0 03	0 10	300	0 33	0 62	1 87	400	0 52	1 04	3 12								
_6	50	0 06	0 37	1 03	200	0 20	0 48	1 47	400	0 35	1 12	3 37								
_3	50	0 14	0 16	0 50	300	0 60	0 79	2 37	400	1 08	1 39	4 17								
_10	48	0 06	0 24	0 73	300	0 08	1 09	3 28	500	0 33	3 44	10 34								
_8	100	0 10	0 37	1 13	200	0 13	0 59	1 78	400	0 23	1 33	3 99								
_14	100	0 07	0 38	1 16	200	0 12	0 55	1 67	400	0 19	1 01	3 03								
_6	48	0 10	0 18	0 56	150	0 21	0 48	1 45	300	0 30	1 17	3 50	400	0 44	1 56	4 74	500	0 63	2 41	7.23
_6	50	0 15	0 20	0 61	200	0 25	0 50	1 49	400	0 59	1 72	3 67								
_10	40	0 06	0 24	0 72	160	0 19	0 79	2 37	280	0 36	1 34	4 02	400	0 68	1 96	5 90				
_9	100	0 12	0 35	1 06	200	0 23	0 77	2 33	300	0 45	1 33	3 99								
_16	100	0 11	0 40	1 19	200	0 26	0 97	2 90	300	0 62	2 35	7 06								
_8	50	0 04	0 25	0 76	150	0 17	0 80	2 39	300	0 47	1 60	4 79								
_10	50	0 13	0 13	0 39	150	0 24	0 46	1 38	300	0 33	1 12	3 37	400	0 71	2 88	8 65				
_16	100	0 11	0 35	1 05	200	0 27	0 86	2 59	300	0 48	1 89	5 67								
_0	50	0 17	0 29	0 89	300	0 36	0 79	2 38	400	0 54	1 74	5 24								
_8	50	0 08	0 12	0 37	300	0 43	0 67	2 01	400	0 64	1 19	3 58								
_0	40	0 13	0 12	0 37	160	0 24	0 25	0 76	280	0 39	0 55	1 65	400	0 77	1 19	3 59				
_10	50	0 17	0 41	1 23	150	0 29	1 01	3 03	300	0 59	2 36	7 13								
_12	42	0 07	0 14	0 41	154	0 17	0 48	1 45	300	0 53	1 32	3 97	395	0 68	1 98	5 94				
_12	100	0 08	0 33	0 98	200	0 28	0 84	2 52	300	0 51	1 54	4 63								
_9	10	0 07	0 05	0 16	110	0 12	0 53	1 59	320	0 50	1 75	3 25								
_5	100	0 16	0 62	1 88	200	0 29	1 03	3 10	400	1 28	3 18	9 56								
_14	50	0 08	0 38	1 14	150	0 29	1 24	3 73	220	0 33	2 29	6 87								
_12	100	0 13	0 40	1 21	200	0 30	1 04	3 12	300	0 41	1 74	5 21								
_7	100	0 13	0 31	0 93	200	0 31	0 71	2 13	300	0 46	1 35	4 06								
_5	35	0 06	—	—	120	0 18	—	—	200	0 44	—	—								
_7	40	0 13	0 12	0 37	280	0 42	0 56	1 68	400	0 86	1 26	3 80								
_2	50	0 17	0 38	1 14	150	0 26	0 54	1 62	300	0 57	1 43	4.29								
_9	40	0 12	0 46	1 40	160	0 29	1 08	3 23	280	0 50	1 39	4 18	400	0 81	4 75	14 25				
_5	40	0 11	0 18	0 53	160	0 27	0 45	1 35	280	0 54	1 08	3 24	400	0 83	1 96	5 89				
_5	50	0 12	0 23	0 71	300	0 63	1 03	3 10	400	1 03	1 82	5 48								
_7	100	0 25	0 86	2 60	200	0 41	1 68	5 06	320	0 85	3 88	11 64								
_11	40	0 11	0 17	0 51	280	0 59	1 09	3 27	400	1 07	2 25	6 75								
_7	40	0 12	0 18	0 55	280	0 63	1 30	3 91	400	1 79	3 18	9 54								
_6	50	0 17	0 25	0 75	200	0 52	0 80	2 40	400	0 90	1 50	4 52								
_7	50	0 08	0 12	0 36	150	0 39	0 69	2 07	330	0 98	1 85	5 54								
_11	50	0 18	0 53	1 60	150	0 36	1 21	3 62	300	0 97	3 17	9 51								
_7	48	0 10	0 16	0 48	150	0 28	0 58	1 74	300	1 09	2 18	6 55	400	1 86	4 26	12 78				
_3	10	0 05	0 06	0 19	110	0 23	0 69	2 07	320	1 14	2 09	6 28								
_7	50	0 17	0 24	0 73	150	0 46	0 74	2 22	330	1 40	2 39	7 18								
_9	50	0 11	0 09	0 27	150	0 52	0 84	2 52	330	1 69	3 21	9 63								
_15	10	0 06	0 02	0 08	110	0 30	0 76	2 29	250	1 11	2 64	7 93								
_16	42	0 12	0 15	0 46	154	0 54	0 66	1 98	300	1 38	1 57	4 72	395	2 10	2 45	7.36				
_11	50	0 22	0 70	2.10	150	0 48	1 29	3 88	300	1 71	3.43	10.35								
_10	40	0 21	0 17	0 53	160	0 54	0 75	2 25	280	3 08	4 13	12 41								
_15	50	0 16	0 29	0 86	150	0 72	1 19	3.58	220	2 92	3 37	10 12								
_10	50	0 20	0 48	1 44	150	0 62	1 43	4 30	300	3.55	5 80	17 41								
_13	35	0 06	—	—	120	1.12	—	—	150	2 44	—	—								
_7	35	0 15	—	—	80	1.01	—	—	120	2 23	—	—								
_8	35	0 45	—	—	50	0 97	—	—	120	5 61	—	—								
_11	5	0 04	0 03	0 09	30	0 21	0 67	2 03	55	1 35	2 56	7.70								
_16	35	0 87	0 86	2 59	70	3.19	4 56	13 67	—	—	—	—								
_13	5	0 06	0 10	0 31	25	0 57	0 93	2 81	50	3 47	5 80	17 40								
"	10	0 18	0 32	0 96	20	0 47	0 93	2 81	40	2 05	3.13	9 38								
"	10	0 23	0 26	0 79	20	0 54	0 70	2 10	40	2 31	2 92	8 76								
"	10	0 20	0 19	0 58	20	0 44	0 67	2 02	40	2 06	2 62	7 86								
_6	35	1 58	—	—	50	4 00	—	—	—	—	—	—								
_8	10	0 47	0 64	1 93	20	1 15	1 83	5 51	—	—	—	—								
_13	5	0 44	0 51	1 53	15	2 05	2 53	7 61	30	8 09	9 77	29 32								
_12	40	4 57	3 85	11 55	—	—	—	—	—	—	—	—								

Figure 34. Test results for concrete with high or very high resistance (disturbance factor < -10).

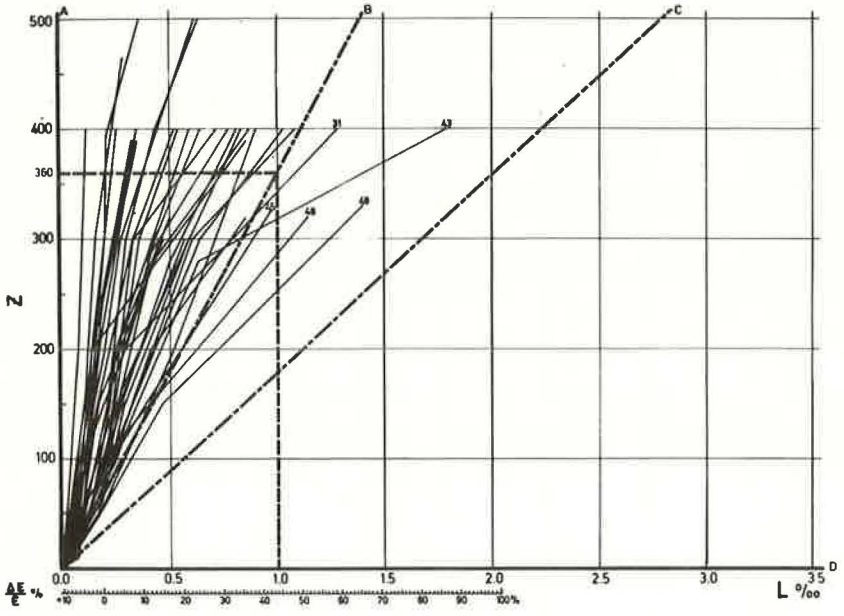

Figure 35. Test results for concrete with high to very high resistance (disturbance factor ≥ 10).

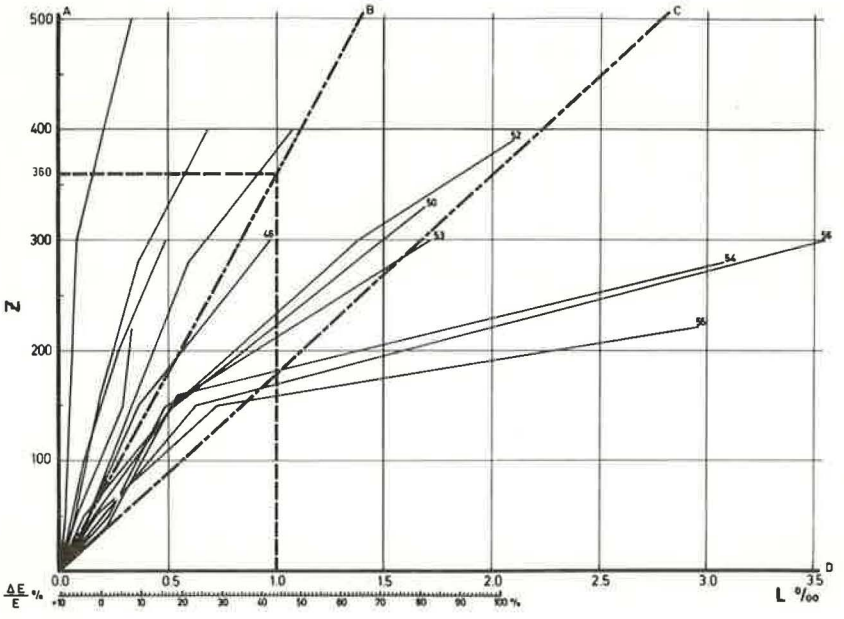

Figure 36. Test results for concrete with medium resistance (disturbance factor = - 5 to -16).

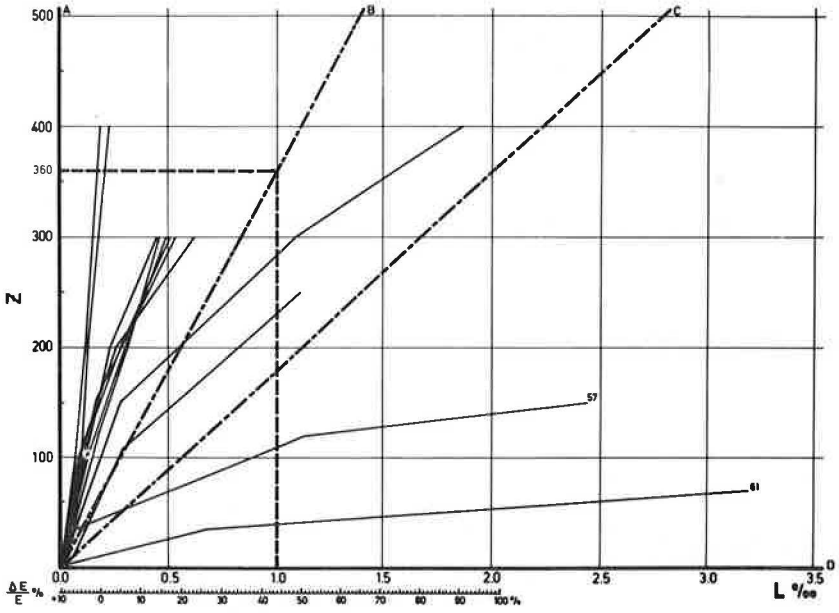

Figure 37. Test results for concrete with low or very low resistance (disturbance factor = -7 to -13).

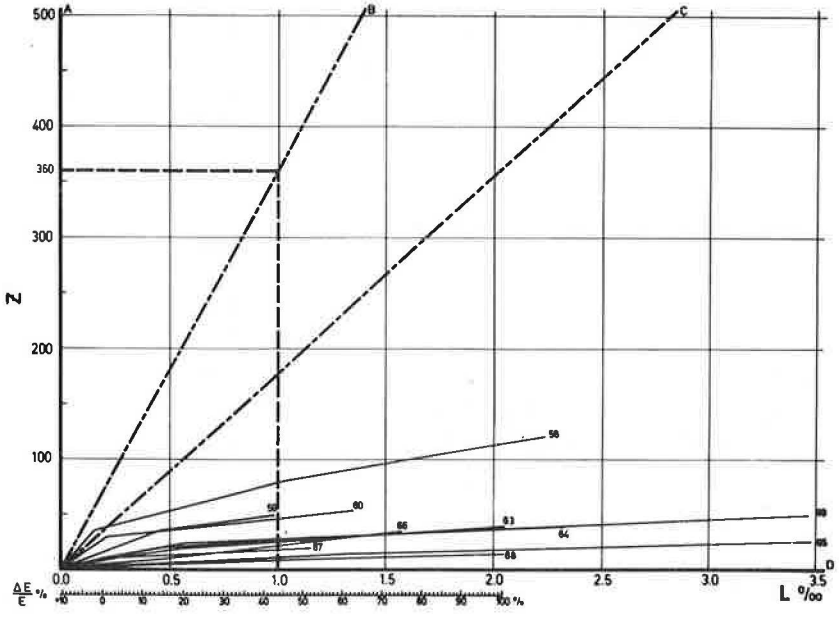

Figure 38. Concretes according to decreasing durability factor.

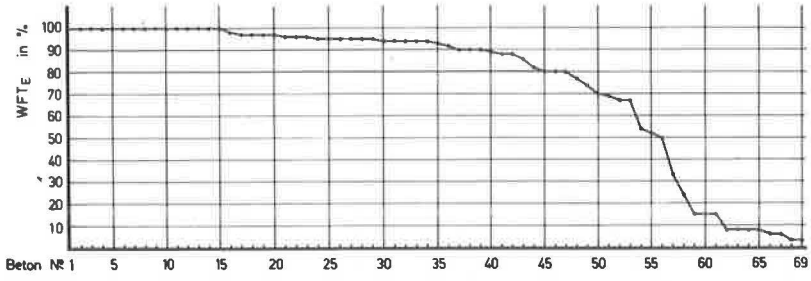

Figure 39. Relation between spacing factors and durability factor.

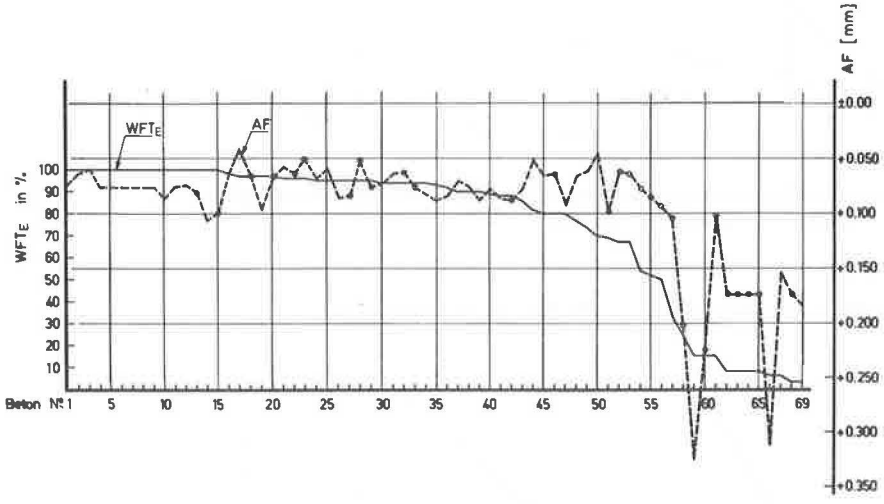

Figure 40. Relation between fine pore contents and durability factor.

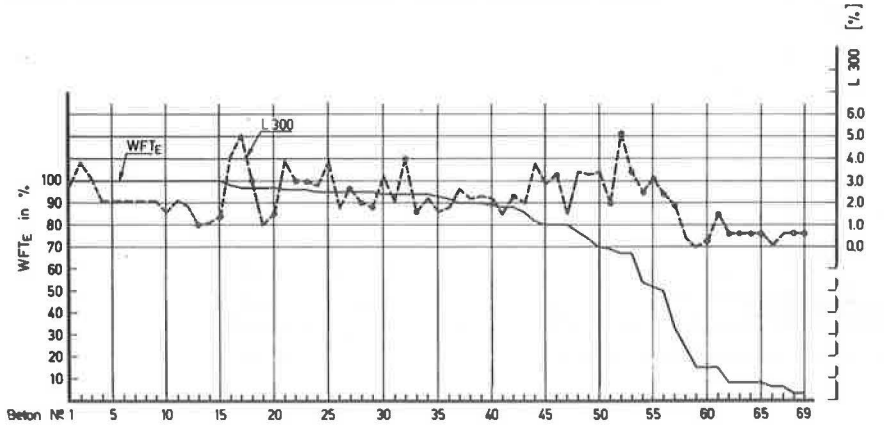

Figure 41. Relation between characteristic value and durability factor.

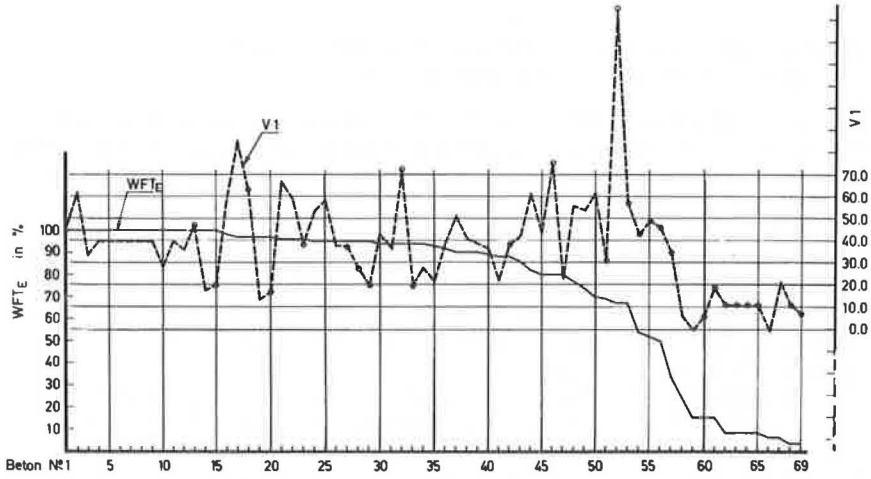

Figure 42. Relation between supplementary value and durability factor.

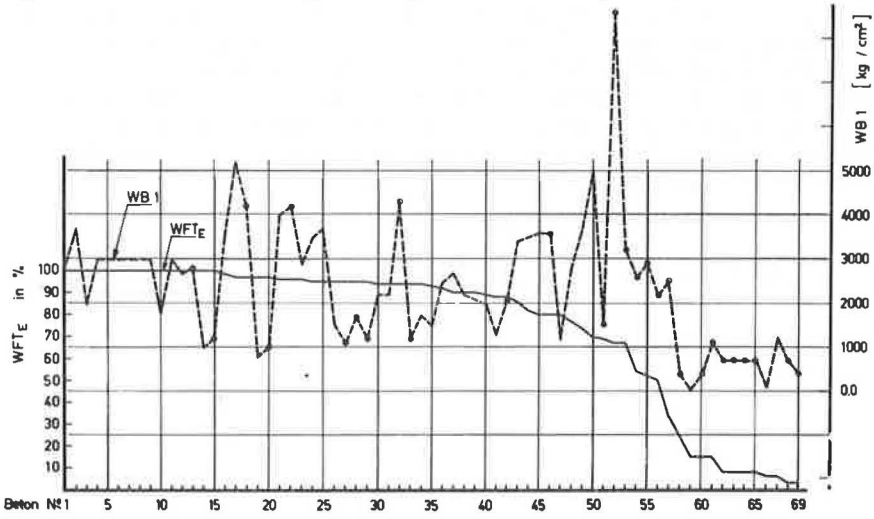

Figure 43. Relation between total air contents and durability factor.

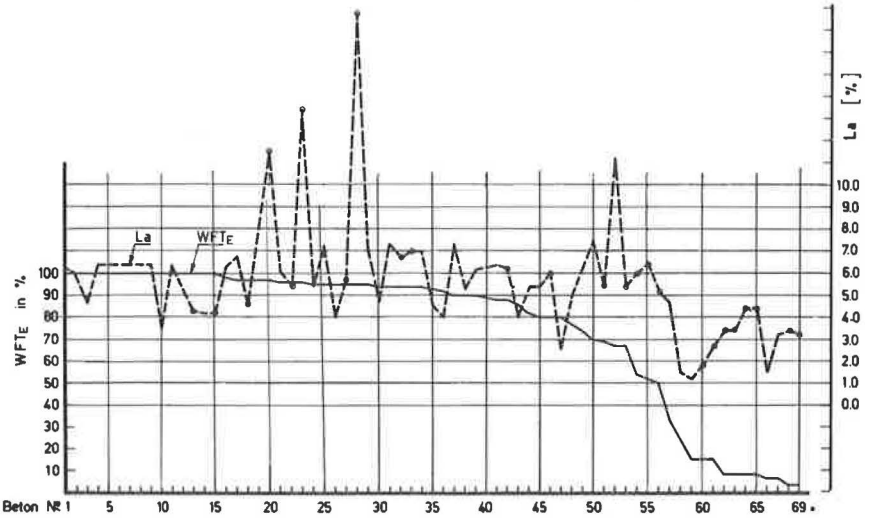

RELATIONSHIP OF F-T-S RESISTANCE AND PORE ANALYTICAL CHARACTERISTIC VALUES

The relationship of durability factor WFT_E (F-T-S resistance) and individual characteristic values (Fig. 33, cols. 8 to 18) can be assessed from results of the 69 concretes tested. WFT_E was determined from F-T-S test results (Fig. 33, cols. 21 to 25) according to ASTM C 666-B.

Figure 38 shows the 69 concretes according to decreasing WFT_E. Figure 39 shows the relationship between the spacing factors AF (col. 12) and WFT_E values. A good connection exists within the range of WFT_E = 100 to 80 percent in which the spacing factor varies between 0.05 and 0.1 mm. In the medium range, WFT_E = 80 to 50 percent, a connection between these variables is less pronounced, and at low WFT_E values, < 50 percent, a wide scattering exists.

Figure 40 shows relationships between fine pore contents L_{300} (col. 9) and WFT_E values. A relatively good interrelation exists within the higher ranges, WFT_E = 100 to 90 percent.

Figure 41 shows the relationship between the characteristic values V_1 (col. 15) and the WFT_E values. A restricted relationship with strong variations of V_1 can be seen in the higher ranges of WFT_E values.

Figure 42 shows the relationship between the supplementary value WB_1 (col. 17) and the WFT_E values. A loose connection exists between the two curves. Figure 43 shows the relationship between total air contents L_a (col. 8) and WFT_E values. A loose association of the two curves exists with strong variations in the L_a values.

Figures 38 through 43 show that an estimate of the F-T-S resistance based on individual characteristic values and even on the spacing factor will have only limited meaning. An essentially stronger determination is achieved when all characteristic values are included in the assessment (Figs. 1, 34, 35, 36, and 37).

REFERENCE

1. Schäfer, A. Deutscher Ausschuss für Stahlbeton. Heft167, 1964.